



VLA OBSERVING APPLICATION

AB 346

received:

SEND TO: Director NRAO Edgemont Rd. Charlottesville, Va. 22901

DEADLINES: 15th of Mar., June, Sept., Dec. for Q 3, 4, 1, 2 respectively

(1) Date: 13 March 1985

(2) Title of Proposal: Low-brightness features of NGC6251

For Grad Students Only					
(3)	Authors	Institution	Who will observe?	Observations for "PhD Thesis?"	Anticipated PhD Year
	A.H. Bridle	NRAO / CV			
	R.A. Perley	NRAO / VLA			

(4) Related previous VLA proposal number: AP66 (request for rescheduling of failed part of AP6)

(5) Contact author for scheduling: R.A. Perley

(6) Telephone:

Address: VLA

TWX:

(7) Scientific category: planetary, solar, stellar, galactic, extragalactic

(8) Configuration(s) (A, B, C, D, A/B, B/C, C/D, Any)	D				
(9) Wavelength (90 20 18 6 2 1.3 cm)	20/6				
(10) Time requested (hours or days)	24hrs				

(11) Type of observation: mapping, point source, monitoring, continuum, lin poln, circ poln,
 spectral line, solar, VLBI, phased array, other

(12) ABSTRACT (do not write outside this space):

We wish to be rescheduled for the part of AP66 which failed due to operations problems with the VLA. The purpose is to examine the spectral gradients and Faraday rotation properties, as well as the magnetic field configuration over the low-brightness regions of the giant radio galaxy NGC6251. We also wish to test Laing's lobe magnetic field model for this source, and to understand why the S symmetry of the jet/confiner does not extend eastwards in the source.

NRAO use only

(13) Observing style: Will be present Will prepare files & Will use modem Absentee (NRAO prepares OBSERV file & return to reduce sends calibrated data)

(14) Reduction: Number of maps 12 Maximum size of maps 512 Self-call maps 12 Private disk pack

15 Off-site reduction: none, post map, post calibration, everything.

(16) Help required: none, consultation, friend (extensive help), staff collaborator.

17) Spectral line only: line 1 line 2 line 3 line 1 line 2 line 3
 transitions to be observed _____ number of channels (N) _____
 channel bandwidth (KHz) (Δ) _____ number of antennas _____
 observing frequency ($\pm N\Delta/2$) _____ rms noise after 1 hour (mJy) _____

(18) Number of sources 1 (If more than 10 sources please attach list. If more than 30 give only selection criteria and LST range(s).)

(19) Special hardware, software, or operating requirements:

(20) Preferred range of dates for scheduling: ..

② Dates which are not acceptable:

(22) Please attach a self-contained Scientific Justification not in excess of 1000 words.

When your proposal is scheduled, the contents of this cover sheet become public information. (Any supporting documents are for refereeing only)

NATIONAL RADIO ASTRONOMY OBSERVATORY
Edgemont Road, Charlottesville

13 March 1985

TO: Paul Vanden Bout

FROM: Alan Bridle, Rick Perley

RE: Rescheduling of VLA D array observations of NGC6251

We wish to apply for rescheduling of the 'D' array segment of our proposal AP66 for mapping the low-brightness lobe features of NGC6251 at 6 and 20 cm with the VLA. This proposal was given time in the 'C' and 'D' array seasons in 1983 but the 'D' array observing was unsuccessful for operational reasons. To support the resubmission we attach the original proposal, and a map from the (successful) 'C' array observations.

AP66 called for 'C' array data mainly to define properties of the outer main jet, the counterjet and lobe fine structure, and 'D' array data mainly to define the spectral, polarization, and rotation measure characteristics over the extended lobe emission. We "piggybacked" an 18cm 'C' array run on a 28-hr VLB observation of NGC6251 which used the VLA in phased array mode; Figure 1 shows a tapered map from this run, at 25" resolution. It clearly demonstrates (a) that the two jets share a distorted S-symmetry, (b) that the counterjet is not a fainter replica of the main jet, but rather that the brightness ratio between the two jets changes with distance from the core, (c) that the "warm spot" in the west lobe shares the S-symmetry of the jet/counterjet system with a corresponding warm spot at a bend in the counterjet. The last result increases the importance of examining the magnetic and spectral properties of the extended emission to the east of the warm spot in the counterjet (Figure 2), as it is now much clearer that the most easterly emission in NGC6251 breaks an underlying S-symmetry in the source. The 'C' array 6cm data (required for better signal to noise on the main jet than achieved in our published work) were also of acceptable quality for our present purposes.

Unfortunately, the 'D' array data requested in AP66, taken in June 1983, are almost entirely useless. The observing run was scheduled just as the BD IFs were being brought into use. Due to various operational problems, the new BD channels were brought up with no delays set, and the AC channel delays were improperly determined. The result was that only the parallel-hand data were useful at 6cm, while at 20cm no valid data at all were obtained. We therefore request rescheduling of the 'D' array segment of this proposal for 12 hrs in the next 'D' array season.

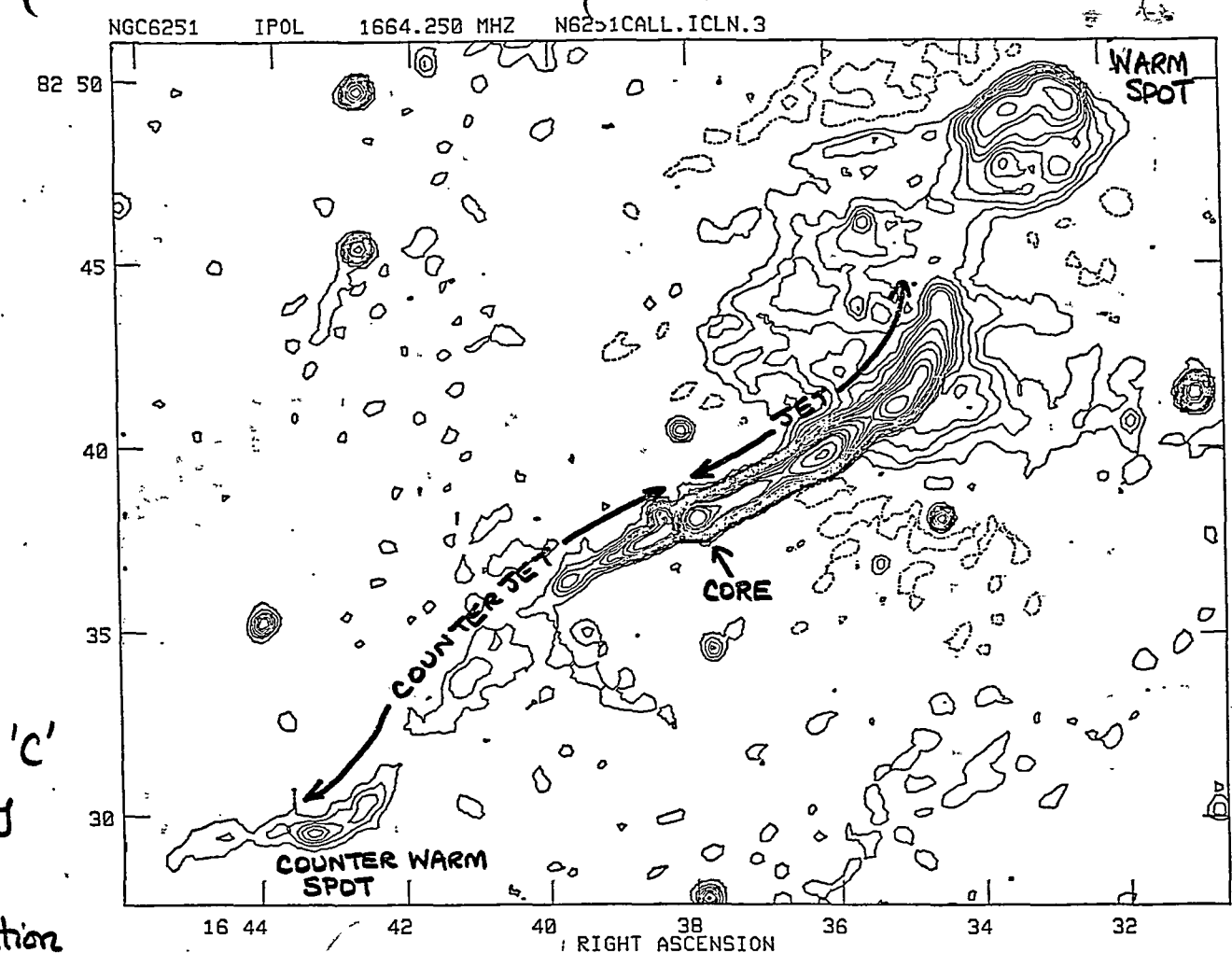


Fig. 1
VLA 'C'
Array

25"
resolution

Al 8cm

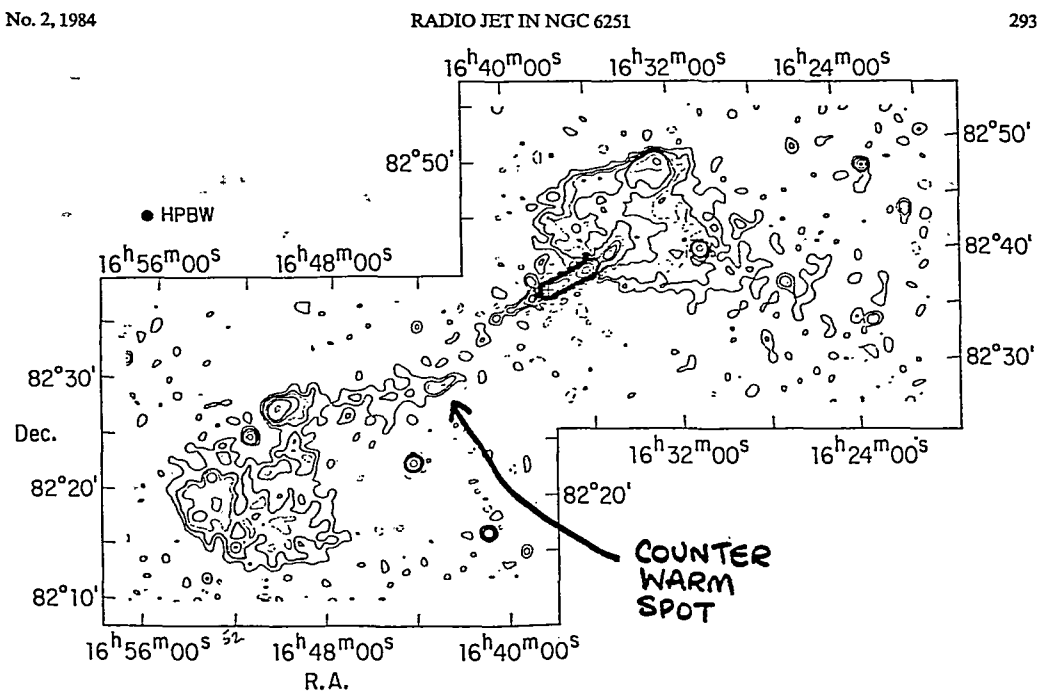


Fig. 1.—Map of the entire NGC 6251 source at 610 MHz with 50" resolution (from Willis *et al.* 1982). The cross marks the position of the nucleus of NGC 6251.

TABLE IA
VLA OBSERVING PARAMETERS

PARAMETER	DATE			
	1979 Nov 05	1980 Mar 31	1980 Dec 05	1981 Oct 05

ORIGINAL PROPOSAL AP66

TO: M.S.Roberts
FROM: R.A.Perley and A.H.Bridle
DATE: 4 October 1982

SUBJECT: Proposal to observe the low-brightness features of NGC6251 at 6 and 20 cm with the VLA in the C and D configurations.

We request the use of the VLA for 24 hrs in each of the C and D configurations to map total and polarized intensities of the counterjet and lobes of the large radio galaxy NGC6251. The proposal is the first of a new program intended to explore aspects of the source revealed by, or related to, our previous study of the bright jet in this object.

BACKGROUND

NGC6251 is a 14th-magnitude elliptical galaxy with a redshift of 0.023 associated with radio source 1.1 degrees in overall extent. For $H=75$ km/s/Mpc the linear diameter of the source is 1.7 Mpc, making it one of the largest known radio galaxies. A high-brightness jet some 120 kpc long was discovered in the source by Waggett, Warner and Baldwin (1977). We observed this jet using the A configuration at 21 and 18cm, a hybrid (construction) configuration at 20 and 6 cm, and a D configuration "snapshot" at 20cm. The main results of these observations were:

1. Evidence that the jet may be interacting with a surrounding medium: it expands in several discrete steps, and exhibits lateral oscillations which are readily interpreted as Kelvin-Helmholtz instability modes of a confined jet.
2. Evidence that the surrounding medium may be an ionized magnetosphere of NGC6251: there are large and complex Faraday rotation gradients over the central parts of the source. These gradients cannot be due to thermal electrons and fields in the jet because there is no significant depolarization between 21cm and 6cm. Rather, the gradients, which are largest closest to the center of NGC6251, must arise in material between us and the jet but associated with NGC6251.
3. Detection in the D array snapshot of a weak counterjet whose intensity within 90" of the core is about 1/40th that of the main jet, but decreases to <1/250th that of the main jet further from the core. The reality of this counterjet is confirmed by a WSRT 610 MHz map at 50" resolution.
4. Mapping of the magnetic structure of the jet in detail: the projected field contains both parallel and perpendicular components, with deep field-parallel layers at the edges of the field-perpendicular configuration in the more expanded outer regions of the jet. There are also regions of oblique projected field which can be explained only if there are departures from axial symmetry in the internal structure of the jet.

These results will soon be submitted to the Ap.J. They raise questions about NGC6251 which we wish to explore using various combinations of frequencies and configurations, now that reduction and interpretation of the earlier data are complete. Some of the new observations require modes of operation or equipment not yet installed at the VLA; these will be requested as the VLA becomes capable of supporting them. This request is for the parts of the ongoing study which can be done now.

STUDIES OF THE COUNTERJET

We wish to determine the internal structure, collimation and polarization

properties of the counterjet, for comparison with those of the main jet. The counterjet is too faint and resolved to be detectable at A or B configuration resolution at 20cm, but is very clear in our D configuration snapshot at this frequency (Figure 1). We require a mixture of C and D configuration observations at 20cm and 6cm to examine its structure in both total and polarized intensities.

The symmetries of its expansion, brightness-width evolution, field configuration and Faraday rotation properties relative to those of the main jet are all potent tests of models for these quantities which depend on the existence of a gaseous halo around the nucleus of NGC6251. The ratio of brightnesses between the counter jet and the main jet as a function of distance from the core source is also an important constraint on theories of the jet/counterjet mechanism. We will combine C and D configuration observations of about 3 hrs duration at 21cm, 18cm and 6cm to address these matters.

THE OUTER REGION OF THE MAIN JET

The parts of the main jet beyond about 5' from the core (see Figure 1), are resolved out in our earlier high-resolution observations but only poorly resolved in the D configuration snapshot at 20cm. Important questions about the transition between the main jet and the northwest lobe cannot be answered using the present data sets. What is the path and brightness evolution of the jet as it enters the northwest lobe? What is the magnetic structure in the region where the jet "ends", presumably sharing its momentum with the surrounding material? Can the jet be traced continuously to the "warm spot" at the northwestern edge of the source, and what is the structure of this warm spot? The latter provides an indirect constraint on the jet velocity; if the jet does reach the warm spot, it presumably has sufficient thrust to overcome the internal pressure of the spot. We therefore require maps of the northwestern lobe with better resolution than at present, but with sufficient short spacings to sample and separate structural scales from 10" to 10' (see Figure 1). We need to combine C and D configuration observations at 20cm and 6cm of at least one more phase center along the probable path of the jet in the northwestern lobe.

ROTATION MEASURE AND SPECTRAL GRADIENTS IN THE LOBES

There is evidence from the Cambridge 151-1417 MHz observations of the lobe that the emission between the bright jet and the northwest warm spot has a spectrum similar to that of the jet, but that the more diffuse lobe emission away from the jet has a spectrum 0.5 steeper. Our data show that there is no significant spectral gradient along the jet and (from the brightness-width evolution) that particle acceleration continues for some tens of kpc along it. We wish to study both the rotation measure and spectral gradients over both lobes for comparison with the large RM gradients and negligible spectral gradients we have established for the jet. The RM data will test our interpretation of the RM gradients in the jet - we expect very little RM gradient over the lobes if the gradients over the jet indeed originate in the inner regions of a magnetosphere of NGC6251. WSRT 610 MHz data show that the lobes are significantly polarized and will be used for comparison with the VLA 20 cm observations. The C configuration observations will provide higher-resolution data for the more compact lobe features at 20cm for comparison with the VLA D configuration data at 6cm. They will also be used to measure the RMs of about five unresolved background sources which are viewed through the lobes.

The lobes of NGC6251 will also be a good arena in which to test the lobe magnetic field model of Laing (1980), wherein the field is sheared so as to be tangential to the surface of the lobe, with no radial component, but is otherwise random. To test this model quantitatively, we need to establish the projected

magnetic field direction over the lobe, and to check for depolarization over it. Previous tests of the model in M84 (Laing and Bridle, in preparation) met with different degrees of success on the two different sides of the same source; again in the presence of large-scale RM gradients believed to be associated with the parent object. NGC6251 is suitable for further tests of the Laing model, as its lobes are bright, two-dimensional structures over which the VLA can map many pixels. To determine polarization structure (with typical degrees of polarization of 20%), 1-hr integrations at 50 MHz bandwidth are required for several phase centers at 20cm. Due to the 1.1 degree size of the source, three separate phase centers are required for the northwest lobe, counterjet, and southeast lobe observations, even at 20cm.

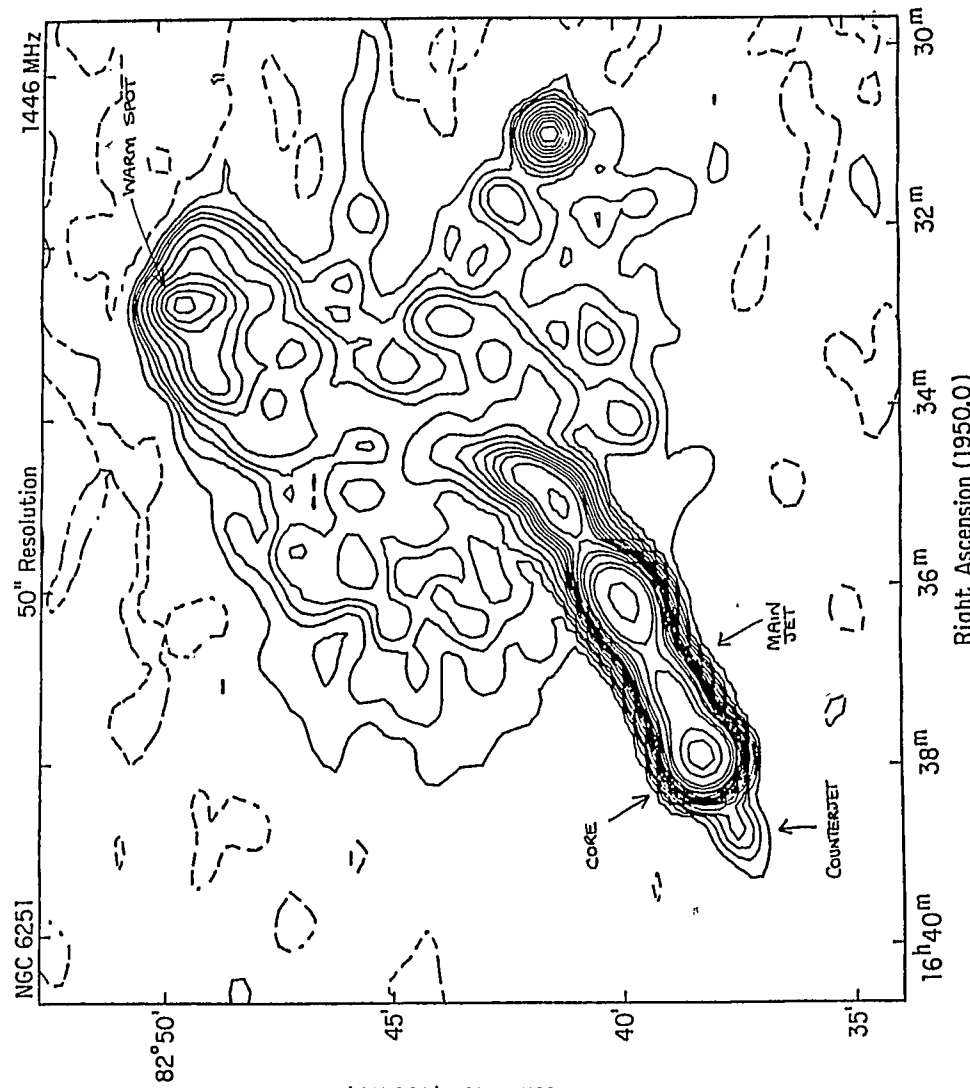
TIME REQUEST

~~~~~

We request 24 hrs in each of the D and C configurations of the VLA for these observations. In the D configuration, we will spend about 1 hr at each of three phase centres at 20cm, and the balance of the time at 6cm. We will be able to specify the time and frequency distribution of the C configuration observations in detail only after the D configuration data are available, but presently estimate our requirement as 24 hrs mainly at 20cm. Due to the 83 degree declination of NGC6251, a single 24-hr run in each configuration is feasible.

#### REFERENCES

- Laing,R.A. 1980. M.N., 193, 439.  
Waggett,P.C, Warner,P.J., Baldwin,J.E. 1977. M.N., 181, 465.



Declination (1950.0)

Figure 1

From: VAX3::RICK 12-JUN-1983 16:00  
To: CVAX::BRIDLE  
Subj: chagrin, embarrassment, shame

I have just scanned our run from last night, and discovered the observe file had a crucial error. The A/C Fluke setting was 12.5 MHz too high, causing the 50MHz passband to contain only 37.5MHz width of data. Fortunately, this only occurred on the calibrator 1803+784. All the observations of NGC6251 are all right, as are the observations of 3C48 and 3C138. It appears that only polarization calibration will suffer, and we'll probably be able to recover that from next week's run.

I cannot explain how this happened. I used SOS to substitute 100.0 and 200.0 (the correct settings) for 112.5 and 212.5 (the old setting used for the C array data). All the 212.5 did change to 200.0 (hence, the B/C

oops, I mean B/D data are o.k.), however, only the 112.5 Fluke settings on cards of the source, 3C48, and 3C138 changed. Somehow, I goofed. Of course, the real error was in the lack of adequate final checking, and for this I am truly sorry. I just hope we can recover the polarization calibration next week.

The operator said he saw no interference. I won't know for sure until tomorrow. I'll make a quick map, and let you know.

From: VAX3::RICK  
To: CVAX::BRIDLE  
Subj: New observations

11-JUN-1983 15:21

I used my two hours of test time to integrate on the following frequencies: 4885, 4835, 1665, 1515, 1485, and 1435MHz. All were pretty clean except 1435 MHz, which had a lot of sporadic RFI, and one scan which was completely blown away. Thus, I believe we should do the following for tonight:

- 1) Observe the core at 4885/4835 MHz. No problem here.
- 2) Observe near the warm spot for 1 hour.
- 3) Observe the core at 1665/1515 MHz.
- 4) Observe the S lobe at 1465/1515 MHz.

In all cases, the more important/more reliable frequency is in the A-C channels. I thought that 2 hours on the core at 6cm, and 1.5 hours at each of the 20cm pairs (S lobe and core) plus the 1 hour at the warm spot should do.

I have been mulling over your comment about deferring the 6cm observations. Sounds good to me from an interference point of view. This (meaning tonight) is a night/weekend run, and much less likely to be zapped

Cancel the above argument which I didn't finish. The long run next week is a midnight run. Nevertheless, given the reliability of the 6cm observations, it makes good sense to test the waters at 20cm now, on a weekend. I'll make up the file at 20cm only, using items 3 and 4 above. I'll split the time equally between the two observations. Any comments?

From: VAX3::RICK  
To: CVAX::BRIDLE  
Subj: New observation

11-JUN-1983 10:04

O.K. I'm at the site. It turns out that I have test time starting in one hour. I plan to tune to these new frequencies, and integrate for a while. Of course, I'll use NGC6251 as the object to integrate upon. The bug in filler which was ruining all the 4-IF data has now been repaired (turned out that the signs of the real and imaginary parts were being reversed), so I can properly calibrate the 2 hours of test data I took on blank sky a couple nights ago. This will tell us the best (i.e. least noisy) frequencies. I'll select the best (subject to careful reading of your comments from yesterday), and integrate on them for a while, to see if occasion RFI lurks about.

More late. Call the operator to get me.

From: VAX3::RICK  
To: CVAX::BRIDLE  
Subj: New obs, and B/D IFs.

9-JUN-1983 10:13

The B/D ifs are here, and they seem to operate. I ran a few hours of tests to find optimal frequencies. The best contiguous frequencies are 1465 and 1515 MHz. An alternative good pair are 1435 and 1485MHz. These have the advantage of averaging close to 1465MHz, the old default frequency. We're observing on Sunday, so we need to consider which pairs we would like. At 6cm, virtually any frequency can be chosen. 4885 and 4835MHz seem to work well.

If, on the other hand, we choose to spread our L-band frequencies, I got good results on any frequency except those which overlap 1600MHz (an enormous internal birdie). I am not in favor of this, however, as we have previously selected (for C array) 'median' frequencies. Furthermore, the noise noticeably increases below 1400MHz. So, I think either 1465/1515 or 1435/1485 are the best bets. Any preferences? Note that the B/Ds seem to work, but there are a few bugs left, such as bad samplers, which seem to cause high closure errors on a few correlators. The situation is similar to the A/C situation a few years ago.

There is a serious bug either in Filler or Antsol which is causing amazing errors in Antsol listings. I am convinced, however, that it is a software problem, and not due to the 4 IFs per se. The data looks good.

As part of the Baars et al experiment that Pat Crane and I are taking care of (checking the Baars flux scale), we have gotten a fair amount of data on 3C274. My summer student arrived yesterday, and I decided to use this data to cut his teeth on the VAX. We got an impressive map of the halo. The remarkable thing is the evidence for rotation of the jet as a function of scale size. I'll send a copy of the map over the wire to you.

How's the review coming? Haven't heard from you in a few days.

For the S lobe, we used 1452.4

jer

1664.25

From: VAX3::RICK  
To: CVAX::BRIDLE  
Subj: RE: Misc. matters

12-APR-1983 18:04

The VL伯 do phase the A and C if-s independently, but so long as they use the same antenna for both, and the true A-C phase of that antenna doesn't change, there should be no problem. The potential problem is that the stupid VLB program may take a different reference antenna each time it phases up. It has some criterion by which it decides which antenna is best, and this criterion or criteria does not account for phase jumps. If there were no phase jumps in any antenna, then changing the reference antenna won't hurt the polarization. The danger is in the phase jumps, and as we all know, phase jumps are rather common here. I don't believe there is any record of which antenna was taken as reference, and of course you know that most phase jumps are invisible to the monitoring system. By the way, self-cal also adjust A and C IFs independently, with no deleterious result to polarization.

The only way I can think of to check the behaviour is to list the AC phases for 1803+784. Pat put in three observations of this source for every observation of NGC6251. Fortunately, 1803+784 has quite a respectable polarization. We should be able to learn a lot from this. Keep your fingers crossed.

To bad about the glossies. Will bribes help? Interesting info about Jennison.

From: VAX3::RICK

11-APR-1983 15:11

To: CVAX::BRIDLE

Subj: More N6251 Observations

Barry has tentatively scheduled our D-array N6251 observations for Sunday, June 19. Are you able to come for these observations, too? Given that we all leave for Italy shortly afterward, it seems reasonable to assume that you won't be able to come. I think it is also reasonable to presume that at that time I'll be frantically working to complete my talk! I notice that you're not listed to give a talk at Bologna. Want some compact source data? Blowing hard today. New storm coming in.

# Jet Velocity estimates in NGC6251

March 1983

## (a) Steady-State Energy Balance

$$F = (U_{\text{int}} + \frac{1}{2} \rho_j v_j^2) v_j \cdot \pi R_j^2 = L_{\text{lobe}} / \epsilon$$

$$\begin{aligned} h &\sim 10^{24} \text{ erg} @ 1480 \rightarrow \\ L_{\text{lobe}} &= 1.1 \times 10^{32} \left( \frac{P_{\text{max}}(\text{Hz})}{\text{W/Hz}} \right)^{0.3} \\ v_{\text{max}} &= 10 \text{ GHz} \end{aligned}$$

$$L_{\text{lobe}} \sim 10^{24} \text{ W/Hz/ster at 1480 MHz} \rightarrow 1.1 \times 10^{35} \text{ Watts.}$$

$$\begin{aligned} \textcircled{4} = 227'' \quad \Delta RM < S &\rightarrow n_e < 2 \times 10^{-4} \text{ cm}^{-3} = 200 \text{ m}^{-3} \\ \rho_j &< 3.35 \times 10^{-31} \text{ kg/cm}^3 = 3.35 \times 10^{-25} \text{ kg/m}^3 \\ U_{\text{min}} &\sim 6 \times 10^{-13} \text{ J/m}^3 \\ U_{\text{min}}/c^2 &\sim 6.68 \times 10^{-30} \text{ kg/m}^3 \\ R_j &\sim 6'' \cdot 5 \sim 2.8 \text{ kpc} \sim 8.6 \times 10^{19} \text{ m} \\ A = \pi R_j^2 &= 2.35 \times 10^{40} \text{ m}^2 \end{aligned}$$

$$\text{Hence: } \left( 6 \times 10^{-13} + \frac{1}{2} \times 3.35 \times 10^{-25} v_j^2 \right) v_j \cdot 2.35 \times 10^{40} = \frac{1.1 \times 10^{35}}{\epsilon}$$

$$1.28 \times 10^{-7} v_j + 3.59 \times 10^{-20} v_j^3 = \frac{1}{\epsilon}$$

|         |                |      |      |      |      |       |      |
|---------|----------------|------|------|------|------|-------|------|
| If:     | $\epsilon = 1$ | 0.1  | 0.05 | 0.04 | 0.03 | 0.01  |      |
| $v_j =$ | 2640           | 6350 | 8080 | 8730 | 9630 | 14000 | km/s |

$$\text{light jet } \frac{1}{2} \rho_j v_j^2 \ll U_{\text{min}} \quad v_j \rightarrow \frac{7801}{\epsilon} \text{ km/s}$$

$$\text{Heavy jet } \frac{1}{2} \rho_j v_j^2 \gg U_{\text{min}} \quad v_j \rightarrow \sqrt[3]{\frac{3031}{\epsilon}} \cdot \left( \frac{3.4 \times 10^{-25}}{\rho_j (227'')} \right)^{1/3} \text{ km/s}$$

$$\textcircled{H} = 32''$$

Defol  $\rightarrow$

$$n_e < 4 \times 10^{-3} \text{ cm}^{-3}$$

$$g_j < 6.7 \times 10^{-30} \text{ kg/cm}^3 = 6.7 \times 10^{-24} \text{ kg/m}^3$$

$$U_{\min} \sim 5.4 \times 10^{-12} \text{ J/m}^3$$

$$R_j \sim 1''75, 0.75 \text{ kpc} \sim 2.31 \times 10^{19} \text{ m}$$

$$A = \pi R_j^2 = 1.69 \times 10^{39} \text{ m}^2$$

$$\text{Hence } (5.4 \times 10^{-12} + \frac{1}{2} \times 6.7 \times 10^{-24} v_j^2) v_j \cdot 1.69 \times 10^{39} = \frac{1.1 \times 10^{35}}{\Sigma}$$

$$8.28 \times 10^{-8} v_j + 5.14 \times 10^{-20} v_j^3 = \frac{1}{\Sigma}$$

|         |                |       |        |        |
|---------|----------------|-------|--------|--------|
| If      | $\Sigma = 1.0$ | $0.1$ | $0.04$ | $0.01$ |
| $v_j =$ | 2490           | 5710  | 7,800  | 12,400 |
|         |                |       |        | km/s   |

$$\text{light jet } v_j < \frac{12000}{2} \text{ km/s}$$

$$\text{Heavy jet } v_j \approx \frac{2690}{\sqrt[3]{\Sigma}} \left( \frac{6.7 \times 10^{-24}}{g_j} \right)^{1/3} \text{ km/s}$$

Suppose we accept expansion rate velocity  $v_j \sim 8000 \text{ km/s}$

$$\Sigma \sim 0.04$$

$$g_j \sim 6.7 \times 10^{-24} @ \textcircled{H} = 32''$$

$$\left. \begin{aligned} \frac{1}{2} g_j v_j^2 &= 2.14 \times 10^{-10} \text{ J/m}^3 \\ U_{\min} &= 5.4 \times 10^{-12} \text{ J/m}^3 \end{aligned} \right\} \underline{\underline{39.7 : 1}}$$

$$v_j \cos i$$

$$\tan \alpha = \frac{v_r}{v_j \cos i}$$

$$= \frac{c_s}{M c_s \cos i}$$

Method (b). Expansion rate.

If the jet is "free" at  $\theta \approx 17^\circ$ ,  $M \approx 14_{\text{seci}}$  there.  $M = \cot \alpha \sec i$

At  $\theta = 17^\circ$ , from BCH fit,  $\frac{f_{17}}{f_{32}} = \frac{0.25}{0.32} = 0.78 \quad f_{17} = 5.2 \times 10^{-24} \text{ kg/m}^3$

From equipartition  $\theta = 17^\circ \quad U_{\min} = 4.4 \times 10^{-12} \text{ J/m}^3$ .

$p_{\min}$  (using  $\times 0.86$  factor)  $\rightarrow 1.26 \times 10^{-12}$

$$\text{Then } c_s = \sqrt{\frac{8f}{g}} = \sqrt{\frac{1.333 \times 1.26 \times 10^{-12}}{5.2 \times 10^{-24}}} = 5.68 \times 10^5 \text{ m/s}$$

$$\text{Hence } v_j = M c_s = 14 \times 5.68 \times 10^5 \text{ seci} \rightarrow 7.95 \times 10^6 \text{ m/s seci}$$

$$\rightarrow \underline{8000 \text{ kn/s. seci}}$$

NB BCH fit itself  $\rightarrow M_{\text{ref}} = 5.4$

$$v_j = \underline{3000 \text{ kn/s.}}$$

### Method (c) . Thrust balance

Warm spot in 50" 1446 MHz snapshot

$$- \text{peak } I = 33.3 \text{ mJy}$$

$$\theta_{\text{obs}} = 1.8 = 108''$$

$$\theta = \sqrt{108^2 - 50^2} = 96'' \text{ intrinsic}$$

$$R_{\text{HS}} = 48'' \rightarrow 20.6 \text{ kpc} = 6.35 \times 10^{20} \text{ m}$$

Assume 0.7 index

$$v \sim 1 \text{ MHz} \rightarrow 1 \text{ GHz} \quad (\text{Same } E \text{ range as jet})$$

$$B_{\text{eq}} \sim 2.6 \times 10^{-6}$$

$$U_{\text{min}} \sim 6.18 \times 10^{-14}$$

$$P_{\text{HS}} A_{\text{HS}} = 0.86 \times \frac{6.18 \times 10^{-14}}{3} \times \pi \times (6.35 \times 10^{20})^2$$

$$= 2.24 \times 10^{28} \text{ Nt.}$$

Momentum flux delivered to lobe is  $f_j f v_j^2 A_j$   $f = \frac{1}{1 + \frac{f_j}{f_{\text{Brem}}}}$

$\Theta = 227''$  parameters

$$\left. \begin{aligned} f_j &= 3.35 \times 10^{-25} \\ A_j &= 2.35 \times 10^{40} \end{aligned} \right\} v_j = 1.69 \times 10^6 \left( \frac{3.35 \times 10^{-25}}{f_j} \right)^{1/2} \cdot \frac{1}{f}$$

$\Theta = 32''$

$$\left. \begin{aligned} f_j &= 6.7 \times 10^{-24} \\ A_j &= 1.69 \times 10^{39} \end{aligned} \right\} v_j = 1.41 \times 10^6 \left( \frac{6.7 \times 10^{-24}}{f_j} \right)^{1/2} \cdot \frac{1}{f}$$

So for  $v_j = 8000 \text{ km/s}$ , need  $f \sim 0.194$   $f_j \sim 17 \text{ SI cm at hotspot.}$

Problem  $P V R^2$

Method (d)

If it's heavy

$$\frac{1}{2} \rho_j v_j^3 A_j = \frac{L_{lobe}}{\epsilon} \quad \text{for energy balance}$$
$$\rho_j \xi^2 v_j^2 A_j = \rho_{HS} A_{HS} \quad \xi = \sqrt{1 + \sqrt{\rho_j / \rho_{IGM}}}$$

$$v_j = \frac{2 L_{lobe} \xi^2}{\rho_{HS} A_{HS} \epsilon}$$
$$= \frac{2 \times 1.1 \times 10^{35} \xi^2}{2.24 \times 10^{28} \epsilon}$$
$$\lesssim \frac{9820 \xi^2}{\epsilon} \text{ km/s.}$$

# NGC 6251 outflow argument.

$$V_j^3 > \frac{2L_{\text{lobe}} d_{\text{hs}}}{\Sigma M_{\text{bit}}}$$

$$1 \text{ yr} = 3.156 \times 10^7 \text{ sec}$$

For Mbar, Reke Faber/Gallagher (ApJ, 204, 365 (1976))

$$\text{Gas ejection rate from sd stars in E galaxy} = 0.013 M_{\odot}/\text{yr} / (10^9 L_{\odot})$$

$$\text{Absolute magnitude of NGC 6251, } M_{B(0)} = -21.3 + 5.48 \text{ Sun}$$

$$\text{Hence } 26.8 = 2.3 \log(L/L_{\odot}) \rightarrow 5 \times 10^{10} L_{\odot} \rightarrow \sim 0.8 M_{\odot}/\text{yr}$$

$$M = TS \rightarrow T_h \sim 1.3 \times 10^{10} \text{ yrs} \rightarrow 10^{10} M_{\odot} \text{ available} \sim 10^{-2} \text{ galaxy?}$$

$$L_{\text{lobe}} = 1.1 \times 10^{35} \text{ Watts} \quad d_{\text{hs}} = 16' = 960'' = 412 \text{ kpc} = 2.7 \times 10^{22} \text{ pc}$$

$$V_j^3 > \frac{1.1 \times 10^{35} \times 1.27 \times 10^{22} \times 2}{\Sigma \times \frac{1}{2} \times 10^{10} \times 3.583 \times 10^{30}} = \frac{1.41 \times 10^{17}}{\Sigma} \quad V_j = 5.2 \times 10^5 \text{ s} / \sqrt[3]{\Sigma} = 5.2 \text{ km/s}$$

$$= \frac{656}{\sqrt[3]{\Sigma}} \text{ km/s}$$

$$\text{For } \Sigma = 0.04, \text{ this gives } V_j > 1640 \text{ km/s} \quad t_j \sim 800 \text{ yr} \sim 6 \times 10^7 \text{ yrs}$$

$$T > 3.1 \times 10^7 \text{ yrs}$$

$$\frac{dm}{dt} \approx 320 M_{\odot}/\text{yr} \text{ (check pers)}$$

$$\text{Note, could have taken over lobe, } d = 38' \rightarrow V_j > \sqrt[3]{\frac{39}{1.1} \times \frac{520}{\sqrt[3]{\Sigma}}} \\ \rightarrow 694/\sqrt[3]{\Sigma} \text{ km/s} \sqrt[3]{\Sigma}$$

What's the optimum set of parameters for heavy N62S1?

We have various estimates:

1) Energy balance       $v_j = \frac{2690}{\sqrt[3]{\varepsilon}} \left( \frac{6.7 \times 10^{-24}}{f(32^\circ)} \right)^{1/3}$  km/s  
 $\textcircled{H} = 32^\circ$

2) ~~Thrust~~ Thrust       $v_j = \frac{1400}{f} \left( \frac{6.7 \times 10^{-24}}{f(32^\circ)} \right)^{1/2}$  km/s

3) Expansion       $v_j = 8000 \sec(i) \left( \frac{5.7 \times 10^{-24}}{f(32^\circ)} \right)^{1/2}$  km/s

4) Mass Flow       $v_j \approx \frac{520}{\sqrt[3]{\varepsilon \Sigma_0}} \left( \frac{5 \times 10^9 M_\odot}{M_{\text{tot}}} \right)^{1/3}$  km/s

To balance energy and thrust we need       $\frac{2690}{\sqrt[3]{\varepsilon}} \approx \frac{1400}{f}$  roughly

$$\underline{\underline{f^3 \approx 0.14 \varepsilon}}$$

So even for  $\varepsilon = 1$ ,  $f$  must be  $\leq 0.52$

This requires  $f_{\text{jer}} \gtrsim 0.9 f_{\text{IEM}}$ .

To balance thrust and expansion we need

$$8000 \sec(i) = \frac{1400}{g}$$

$$\underline{g = 0.18 \sec(i)}$$

This is much harder, and requires  $g < 0.18$

$$\text{i.e. } f_j > 20 \times f_{ISM} !!$$

This is a big problem. It means we must have underestimated  $f_{ISM}$  somehow, if it's in pressure equilibrium. Either the hot spot is far from equipartition, or we have got very bad parameters for it.

As  $v_j \sim \sqrt{f_{ISM}}$ , increasing  $v_j$  by a factor 5 corresponds to increasing  $f_{ISM}$  by a factor  $\sim 25$ . This hot spot is  $\sim 1/25$  the pressure we would have expected.

To balance energy budget and expansion

$$\frac{2690}{\sqrt[3]{\Sigma}} \sim 8000 \sec i$$

$$\underline{\Sigma \sim 0.04 \sec^3 i}$$

$$\cos^3 i @ 10^\circ = 0.96$$

$$20^\circ \quad 0.83$$

This is the constraint we had in the draft paper, with  ~~$i=0^\circ$~~ .

Putting this in mass flow,

$$\frac{0.0656}{0.34 \cos i \sqrt[3]{\Sigma}} \left( \frac{5 \times 10^9 M_\odot}{M_{tot}} \right)^{1/3} = \frac{8000}{\sec i}$$

$$(0.24)^3 = \frac{1.4 \times 10^{-2}}{\cancel{0.0656}} = \frac{\Sigma M_{tot}}{5 \times 10^9 M_\odot}$$

So

$$\boxed{7.0 \times 10^7 M_{\odot} = \Sigma M_{\text{tot}}} \quad \begin{matrix} \text{minimum} \\ \text{- ejected mass.} \end{matrix}$$

$\epsilon_0 \sim 0.1$  ?

$$\underline{M_{\text{tot}} \sim 3.5 \times 10^8 M_{\odot}} \quad \begin{matrix} \text{fuel available} \end{matrix}$$

Things would be much simpler if we had a value for  $\rho_{\text{HS}} A_{\text{HS}}$  that was  $\sim 25 \times$  greater.

or if the jet had been decelerated by a factor of five between the  $\sim 227''$  region and the hot spot.

So if the scale is ~ correct, need  $f^{4/7} \sim (1/25)$   
 $f \sim 0.0036$  !

i.e. There has to be something much smaller out there containing most of the flux ?

Suppose we let  $v_j = 8000 \text{ km/s}$   
 $\xi = 0.04$

At  $\Theta = 32''$   $\frac{dm}{dt} = g_j v_j A_j = 6.7 \times 10^{-24} \times 8 \times 10^6 \times 1.69 \times 10^{39}$   
 $(1 \text{ M}_\odot/\text{yr} = \frac{1.989 \times 10^{30} \text{ kg}}{3.156 \times 10^7 \text{ sec}} = 6.30 \times 10^{22} \text{ kg/s})$   
=  $9.06 \times 10^{22} \text{ kg/s}$   
=  $1.44 \text{ M}_\odot/\text{yr}$

$\Theta = 227''$   
=  $3.35 \times 10^{-25} \times 8 \times 10^6 \times 2.35 \times 10^{40}$   
=  $1.00 \text{ M}_\odot/\text{yr.}$

Suppose we set

$$\cancel{\rho_{\text{IEM}}} \rho_{\text{IEM}} V_{\text{HS}}^2 \sim p_{\text{HS}}$$

$$\rho_{\text{IEM}} \sim 10^{-26} \text{ kg/m}^3$$

$$p_{\text{HS}} \sim \frac{0.86 \times 6.18 \times 10^{-14}}{3} = 1.77 \times 10^{-14}$$

$$\text{then } V_{\text{HS}}^2 = 1.8 \times 10^{12}$$

$$V_{\text{HS}} = 1.3 \times 10^6, \text{ or } 1300 \text{ km/s.}$$

So there is no difficulty providing ram pressure for confinement at this density.

## Synchrotron scales.

Inner jet  $B \sim 25 \mu\text{gauss}$   $5\text{GHz} \rightarrow 3.5 \times 10^9 \text{ eV}$   $T_{\text{synch}} \sim 3.79 \times 10^6 \text{ yrs.}$

$$\begin{aligned} \text{At } 8000 \text{ km/s, } T_{\text{synch}} &\text{ is } 9.57 \times 10^{20} \text{ metres} \\ &\sim 3.1 \times 10^4 \text{ pc} = 31 \text{ kpc} = \underline{\underline{72''}} \end{aligned}$$

Outer jet  $B \sim 7 \mu\text{gauss}$   $5\text{GHz } T_{\text{synch}} \sim 2.56 \times 10^7 \text{ yrs.}$

$$\begin{aligned} \text{At } 8000 \text{ km/s, } &\rightarrow 6.46 \times 10^{21} \text{ metres} \\ &\rightarrow 2.1 \times 10^5 \text{ pc} \\ &\rightarrow 488''. \end{aligned}$$

Therefore not surprising that we see no spectral gradients, as even if all  $5\text{GHz}$  particles had been generated at  $\frac{h}{10''}$ , we could transport them out at 8000 km/s slightly further than we see them due to synchrotron losses.

## Deflection of NGC6251 jet.

What angle does it deflect through?

Radius of curvature from the WRT mfp is  $\sim 10' \sim 600''$   
 $\sim 257 \text{ kpc}$

$$r_c = 257 \times 3.08 \times 10^{19} \text{ m.}$$

$$v_j = \sqrt{\frac{S_{\text{ISM}} r_c}{\rho_j h}} v_g$$

Inside the 30 kpc scale ISM  $r_c = \text{large!}$  (jet straighter)

Outside,  $h \sim \text{djet} \sim 16''$

$$v_j = v_g \sqrt{\frac{S_{\text{ISM}}}{\rho_j}} \cdot \frac{600}{16} \sim 6v_g \sqrt{\frac{S_{\text{ISM}}}{\rho_j}}$$

Using our estimates, we have  $S_{\text{ISM}}/\rho_j \sim 3$ ?

$$\underline{v_j \sim 10 v_g}$$

Don't know  $v_g$ , but unlikely to be  $\gg 1000 \text{ km.s}^{-1}$

$$\underline{v_j \sim 10,000 ?}$$

If we used  $h \sim \text{jet diameter or } \underline{\text{hor. spw.}}$   $h = \underline{96''}$

$$v_j = v_g \sqrt{\frac{S_{\text{ISM}}}{\rho_j} \cdot \frac{600}{96}} = 2.5 \sqrt{\frac{S_{\text{ISM}}}{\rho_j}} v_g$$

Re your comments on the power spectra:

Indeed the angle data generally give better spectra (in terms of significant peaks) than the deflection data. This is an important point, as it means that the deflections ARE growing with distance from the core, in general.

When estimating significance, it is important to compare spectra at the same resolution. The only spectra whose significance should be judged from the Gaussian-noise spectrum at the front of the ones I sent you are the 256-resolution spectra. The reason why the 0.19 r.u. peak in the first spectrum looked puny is because that was a 128-resolution spectrum. It looks o.k. compared with the noise spectrum at its resolution (which, of course, I didn't send you!).

I don't know what to make of the broader peaks. They usually resolve at higher resolution into numbers of smaller peaks. I tend to think we should look at the peak excursions from the LOCAL MEAN LEVEL in the power spectrum, in which case these broad peaks are not as significant. Certainly they correspond to "things" in the spectra, whether real oscillations or not, which are not simple harmonic in the way that naive Kelvin-Helmholtz modes would be. I have therefore focused more on the "sharp" peaks so far.

The coming and going of peaks as we vary the distance range is not surprising - I could pick some small distance ranges out of the data and really blow up individual spectral peaks - e.g. the 31" oscillation at the beginning of the "outer" jet. In general I feel happier about spectra which exclude the angle data from the first 10" or so from the core, where we have those very rapid oscillations that decay away. These are obtained by dividing very small deviations by very small distances, and I am suspicious about their reality. Pity we can't carry the errors in individual points through the power spectrum analysis. I do feel the spectra with the close-in angle data excluded are more trustworthy, though.

The "averaged angle" plots are from data where I first plotted all of our results at different resolutions on the same scale (as in the Figures for the paper), then drew an "average" curve through by eye. That curve was then read off every 2" along the jet to get the data whose power spectra were shown. This is o.k. over a limited range of distances from the core - otherwise the effective resolution of the data varies somewhat even though its angular spacing doesn't.

I'll do some more quantitative things regarding statistical significance, then get back to you with revised text and some more power spectrum examples.

I'm starting to revise the Discussion section now. One of the first things I looked at is whether the Chan-Henriksen model we fitted should in fact have "detached" from the confining pressure according to Bob Sanders' criterion. According to his power-law expression it should have done, but according to the detailed criterion (local expansion velocity becoming locally supersonic) it shouldn't. I think the difference lies in the fact that his criterion as given in his paper is in fact only ASYMPTOTICALLY correct. In the 'real' jet, the external pressure changes before the jet has had TIME (distance from the core) enough to detach. I am therefore happier about our use of the CH model than I was when I talked to you from Queen's, but will look into this some more. What is clear is that if the nozzle was somewhat lower than we have modelled it, the jet might have detached sooner and therefore got into the situation where it became supersonic

time we hit it with the "halo" pressure - generating the reconfinement shocks that Bob's paper was basically about. More to follow as I think it through and do a small number of further sums.

I got a letter from Jean-Luc Nieto with preprints of his NGC6251 paper, which has been rejected once. His pictures certainly don't show very much in the form he sent them to me, but he says he has some more observing time coming up soon, and we will keep in contact.

More ski holidays, eh ? Enjoy it while you can !

From: VAX3::RICK  
To: CVAX::BRIDLE  
Subj: n6251

3-FEB-1983 16:00

I have received your message, and am about to print the new version. I have looked over the deflection spectra and must confess that I'm a little worried about the changes in the significance of the peaks. For example, in the second plot (1.3" data, all distances), do we consider the broad peaks at 0.33 and 0.45 reciprocal units significant? They (especially the former) are almost as significant as the marked peak at 0.19 units (5.8"). Furthermore comparing to the Gaussian noise plot above, none of the peaks seems big enough. Use of 256 resolution does seem to help, though as the next plot (#3) does seem to enhance the "proper" peak at 0.19 r.u. (reciprocal units). Looking through the remaining plots, I notice that the last three (all at 2" separation) show interesting differences. The second of these shows a semi-significant peak at 0.32 r.u. This peak also shows up in the first of these three plots, although at a lower level. However, the last of these plots has no trace of said peak - in fact, there's an enormously deep trough! It seems that restriction of the range has made a great difference. This last plot is by far the most convincing in terms of the significance of the various peaks we have previously identified. By "averaged angle", do you mean that the points are averages of nearby measured values?

It seems to me that the angle data gives a better spectrum than the deflection data.

To Rick S Feb 83

Some further power spectrum thoughts -

I tried a set of different Gaussian random number streams, each 100 points long, with the power spectrum analysis program at 256 resolution. All of them gave basically similar "phony peak" statistics. Features of width several channels and peak amplitude five or more times the average of surrounding channels cropped up about five times per spectrum. Similar features with peak amplitude seven or more times the average of surrounding channels cropped up once per spectrum. We could therefore be pretty sure of anything that was as much as eight or nine times the surroundings, very sure of anything ten times the surroundings. I'll go through my individual 6251 spectra now and see which ones survive the test.

They're forecasting snow here now. We shall see.

# TEST

Book No. .... of Books

(SURNAME FIRST)

me

bject .....

Section

NGC 6251 X-ray luminosity [from Bill Ku's 22,000<sup>s</sup> of Einstein IPC data]

$$z = 0.023, H_0 = 75 \text{ km/s/Mpc} \rightarrow D = 92.4 \text{ Mpc} = 92.4 \times 10^6 \times 3.0856 \times 10^{18} \text{ cm} \\ = 2.853 \times 10^{26} \text{ cm}$$

"Nuclear" X-ray source is  $1.4 \times 10^{-12} \text{ erg/cm}^2/\text{sec}$  [0.5-4.5 keV] - IPC.

$$L_X = 1.4 \times 10^{-12} \times 4\pi \times [2.853 \times 10^{26}]^2 \\ = 1.4 \times 10^{42} \text{ erg/s.}$$

Halo is  $\lesssim 15\%$  =  $2.1 \times 10^{41} \text{ erg/s.}$  ( $\sim 5'$  radius), i.e.  $\sim 154 \text{ kpc}$  radius.

Minimum jet pressure =  $0.86 p_{eq}$ , hence  $n_{min} = 0.86 n_{eq}$  for confinement, given T  
 $L_{min} = 0.74 L_{eq}$  -----.

Taking our old "halo" values

$$T = 4 \times 10^7 \text{ K} \\ L_X \text{ was } 2.0 \times 10^{42} \rightarrow \frac{1.5 \times 10^{42} \text{ erg/s.}}{\text{within } 50 \text{ kpc (116")}}$$

Angular resolution of IPC is:  $39''$  for 0.5-4.5 keV, i.e. 42 kpc.

Hence their "nuclear source" is our core + some halo.

Q. How much of our halo is well inside IPC "beam"?

cf M87 ~  $1.5 \times 10^{43} \text{ erg/sec}$

Table 4

0.5-4keV luminosity and mass of media  
required to confine NGC6251 jet

Assumed isothermal Temperature

|  | $4 \times 10^7 \text{ K}$ | $2 \times 10^7 \text{ K}$ | $10^7 \text{ K}$ |
|--|---------------------------|---------------------------|------------------|
|--|---------------------------|---------------------------|------------------|

|        |                            |                      |                                    |
|--------|----------------------------|----------------------|------------------------------------|
| "HALO" | $L_x = 2.0 \times 10^{42}$ | $6.7 \times 10^{42}$ | $1.6 \times 10^{43} \text{ erg/s}$ |
|--------|----------------------------|----------------------|------------------------------------|

|  |                          |                      |                              |
|--|--------------------------|----------------------|------------------------------|
|  | $M = 1.8 \times 10^{11}$ | $3.6 \times 10^{11}$ | $7.1 \times 10^{11} M_\odot$ |
|--|--------------------------|----------------------|------------------------------|

|        |                            |                      |                                    |
|--------|----------------------------|----------------------|------------------------------------|
| "CORE" | $L_x = 7.0 \times 10^{43}$ | $2.3 \times 10^{44}$ | $5.6 \times 10^{44} \text{ erg/s}$ |
|--------|----------------------------|----------------------|------------------------------------|

|  |                       |                   |                           |
|--|-----------------------|-------------------|---------------------------|
|  | $M = 1.9 \times 10^9$ | $3.8 \times 10^9$ | $7.6 \times 10^9 M_\odot$ |
|--|-----------------------|-------------------|---------------------------|

90% of the predicted X-ray luminosity would originate within 50 kpc of the center of NGC6251 for the "halo" component, and within 1 kpc for the "core" component

Divide luminosities by 1.352

$M_{87} \sim 1.5 \times 10^{43}$

Table 5

Parameters of field models fitted to transverse intensity and polarization profiles  
 (see figure 30)

|                                                 | $\Theta = 32''$ | $\Theta = 227''$              |
|-------------------------------------------------|-----------------|-------------------------------|
| Field Pitch angle $\psi_R$                      | $48^\circ$      | $14^\circ$                    |
| Inclination of jet to sky                       | $50^\circ$      | $40^\circ$                    |
| Random field magnitude                          | $0.75 B_0$      | $0.35 B_0$                    |
| Relativistic particle distribution (density)    | Uniform         | Gaussian<br>$\sigma = 0.94 R$ |
| Relativistic particle distribution (pitchangle) | Isotropic       | Isotropic                     |

Mass in the basic RM medium.

ARM  $\sim 70 \text{ rad/m}^2$  across  $L \sim 70'' \sim 30 \text{ kpc}$ .

$$\text{So: } RM = 8.1 \times 10^5 \times \bar{n}_e \times 10^{-6} B_{-6} \times 30 \times 1000$$

$$\bar{n}_e = 0.00288 \text{ cm}^{-3}$$

$$\bar{\rho}_e = \bar{n}_e m_p \sim 4.818 \times 10^{-24} \text{ kg/m}^3$$

$$M = \frac{4}{3}\pi \bar{\rho}_e R^3$$

$$= \frac{4}{3} \times \pi \times 4.818 \times 10^{-24} \times (3 \times 10^4 \times 3.0857 \times 10^{16})^3$$

$$= \frac{1.60 \times 10^{40}}{B_{-6}} \text{ kg}$$

$$= \frac{8.0 \times 10^9 M_\odot}{B_{-6}}$$

27 September 1982

Check Rick's  $\Delta RM$  limit to  $n_e$ .

Take  $\textcircled{H} \sim 240^\circ$   $\Delta RM < 5 \text{ rad/m}^2$

$$B_{eq} \sim 9 \times 10^{-6} \text{ gauss}$$

$$\textcircled{D} \sim 14'' \sim 6000 \text{ pc}$$

$$RM = 8.1 \times 10^5 n_e (\text{cm}^{-3}) B (\text{gauss}) L_{pc} \text{ rad/m}^2$$

$$n_e < \frac{5}{8.1 \times 10 \times 9 \times 10^{-6} \times 6000} < 1.1 \times 10^{-4} \text{ cm}^{-3} \quad \checkmark$$

If  $B_{\parallel} \sim B_{\perp} \sim B_{eq}$ !

Try actual CH config.?  $\textcircled{H} = 227^\circ$

From the CH fit, FWHM of convolved jet =  $42.4 + 27.7 = 70.1$  units

normalisation of compare units is  $\frac{1}{70.1} \times 13.4 \times 0.429 \text{ kpc}$

$$= 0.082 \text{ kpc/cell} = 82 \text{ pc/cell}$$

$$\text{Now put } B_{eq} \sim \sqrt{\overline{B}_{CH}^2 + B_{rand}^2} \sim \sqrt{\left(\frac{1}{2} B_0\right)^2 + (0.35 B_0)^2} \\ = 0.61 B_0 = 9 \times 10^{-6} \text{ gauss}$$

$$B_0 = 14.7 \times 10^{-6} \text{ gauss.}$$

$$\text{Hence } ROT = 8.1 \times 10^5 n_e (\text{cm}^{-3}) \times 0.04 \times 14.7 \times 10^{-6} \times 82 \\ = 39.05 n_e$$

$$ROT = 0.0075 \equiv 1.9 \times 10^{-4} \text{ cm}^{-3}$$

Out at  $\theta \sim 227$

$$n_{eT} \sim 2 \times 10^3 \quad [\text{from the pressure curve fit to confinement}]$$

$$\bar{n} \sim 3 \times 10^{-7} \sim n_e \sim \frac{2}{3} \times 10^{-4}$$

$$\sim 6 \times 10^{-5} \text{ cm}^{-3}$$

[we used this for  $\theta = 240^\circ$ ]

Fick's farcd. est is  $< 1.4 \times 10^{-4} \text{ cm}^{-3}$ . OK

From the equipartition sum,  $n_{eT} \sim 1 \times 10^4$  between  
in the knots,  $\sim 2$  higher  
within them

$$\rightarrow n_e \sim 3 \times 10^{-4} \text{ cm}^{-3}$$

Correct to minimum from the "min. pers. cylinder" calculation [Over/Burns]?

19 Aug 1982

Analysis of JEFFX output on "NGC6251"  $H = 32^{\circ}$ .

The parameter we specify is ROT

$$\text{FARAD} = \text{ROT} * \text{NCO} * \text{BPARL} * W / \cos I \quad (\text{radians}).$$

i.e. if  $r$  is the Faraday depth of a cell 1 unit thick

$$n_e = n_e(\text{max})$$

$$B = B_R \text{ (max at edge of jet)}$$

All Faraday depths then scale to this.

$$\text{ROT} = 8.1 \times 10^5 n_e(\text{cm}^{-3}) \lambda_{\text{metres}}^2 B(\text{gauss}) [\text{Lengths along l.o.s. in pc}]$$

$$\text{Cellwidth } W = 4R / (2NL - 1) \quad \text{Now } NL = 1301$$

$$R = 60$$

$$W = 0.0922 \quad 1301 \text{ of them} \rightarrow \text{Total depth of } \underline{120} \checkmark$$

Now from the CH fit, FWHM of convolved jet =  $47 + 49 = \underline{96 \text{ units}}$

i.e. the normalisation here is that compute units are  $\frac{1}{96} \times 3.75 \times 0.429 \text{ kpc}$

$$= 0.01676 \text{ kpc}$$

$$= \underline{\underline{16.76 \text{ pc}}}$$

$$\text{Now put } B_{\text{eq}} \sim \sqrt{B_{\text{CH}}^2 + B_{\text{rand}}^2} = \sqrt{\left(\frac{1}{2} B_0\right)^2 + (0.75 B_0)^2} = 0.90 B_0$$

$$B_{\text{eq}} = 2.4 \times 10^{-5} \text{ gauss}$$

$$B_0 = 2.67 \times 10^{-5} \text{ gauss.}$$

$$\text{Then here } ROT = 8.1 \times 10^5 n_e (\text{cm}^{-3}) \times 0.04 \times 2.67 \times 10^{-5} \times 16.76 \\ = 14.5 n_e .$$

$$\text{Hence } ROT = 0.02 \quad n_e = 1.38 \times 10^{-3} \text{ cm}^{-3} \quad 37\% \rightarrow 10\% \text{ over profile} \\ \Delta PA \quad 23^\circ \rightarrow -17^\circ = 40^\circ /$$

$$= 0.04 \quad 2.75 \times 10^{-3} \text{ cm}^{-3} \quad 37\% \rightarrow 1\% \\ \Delta PA \quad 28^\circ - 34^\circ \quad 61^\circ$$

[beginning of the first bounce]

$$= 0.06 \quad 4.13 \times 10^{-3} \text{ cm}^{-3} \quad 32\% \rightarrow 7\% \\ \Delta PA \quad 57^\circ - 66^\circ \quad \underline{123^\circ !}$$

[well-developed bounce]

$$= 0.10 \quad 6.89 \times 10^{-3} \text{ cm}^{-3} \quad \text{All} < 20\% \\ \text{This is } \underline{\text{not seen}} \quad \Delta PA \quad +70^\circ, -90^\circ \text{ noisy } \underline{160^\circ !!}$$

If we had used Croft & Jones (1980) we would have concluded that for  $D > 0.8$  we would need  $f_c \leq 2.6$

i.e., in their units  $2fR < 2.6$

$$f = 1600 n_e B \lambda^2 \text{ rad/m}^2/\text{kpc}$$

i.e.  $1600 n_e B \lambda^2 \cdot (1.61) < 2.6$

$$n_e \leq \frac{2.6}{1.61} \times \frac{1}{24 \times 0.04} \times \frac{1}{1600}$$

$$< 1.1 \times 10^{-3} \text{ cm}^{-3}$$

Suppose we had done it from the slab model as for NGC315 in Willis et al. (1981).

$$D \sim \frac{\lambda_2^2}{\lambda_1^2} \frac{\sin(RM\lambda_1^2)}{\sin(RM\lambda_2^2)}$$

$$RM = 8.1 \times 10^5 n_e (\text{cm}^{-3}) B (\text{gauss}) L^{-\frac{1}{2}} \text{ rad/m}^2$$

We want  $D > 0.8$  (say).  $\lambda_2 = 6 \text{ cm}$   $\lambda_1 = 20 \text{ cm}$   $D = 9 \times 10^{-2} \frac{\sin(RM\lambda_1^2)}{\sin(RM\lambda_2^2)}$

If ~~RM~~  $RM = 8.1 \times 10^5 n_e \times \frac{2.4 \times 10^{-5}}{\sqrt{3}} \times 1610 = \frac{1.81}{3+5} \times 10^4 n_e (\text{cm}^{-3})$

Then  $n_e = 10^{-4} \rightarrow RM = \cancel{1.81}$

$n_e = 10^{-3} \rightarrow RM = \cancel{18.1}$

So we would have concluded that  $D > 0.8$  needs  $n_e \geq \cancel{1.6 \times 10^{-3}}$ ?

$$RM = 28.4$$

This would be  $\sim \cancel{x}$  less than we got from the randomized CH sum.

If we used  $n_e = 4 \times 10^{-3} \text{ cm}^{-3}$  here, we would get  $RM = 125.2$

$$\underline{D = 0.2 !!}$$

Conclude from these simulations that  $n_e(32'') \lesssim 4 \times 10^{-3} \text{ cm}^{-3}$

We used  $n(240'') = 6 \times 10^{-5}$

$$\rightarrow n(32'') = 26.5 \times 6 \times 10^{-5} \text{ from BCH ratios}$$
$$= 1.6 \times 10^{-3} \checkmark$$

$\therefore$  we are OK for Hardee.

cf. Slab approach  $n < \frac{1.6}{\cancel{2}} \times 10^{-3}$

Cioffi/Jones  $n < 1.1 \times 10^{-3}$

NGC 6251 " 1'' resolution "

1662 MHz

$D = 92.4 \text{ Mpc}$

$\alpha = 0.7$

$10M_{\odot} \rightarrow 10G_{\odot}$

VAX-fitted slice terms

$\times 10^{-6} \rightarrow \mu$

gauss  $\text{Jm}^{-3}$   $\text{m}^{-3}\text{K}$

| SLICE | $\theta(^{\circ})$ | $I_{\max}$ | $\bar{\theta}(^{\circ})$ | $\bar{\theta}_0$ | $\Delta(^{\circ})$ | $B_{eq}$    | $U_{min}$                           | $nT_{eq}$ |
|-------|--------------------|------------|--------------------------|------------------|--------------------|-------------|-------------------------------------|-----------|
| 1     | 0                  | 41.9       | 1.413 ± .04              |                  | -0.0004            |             |                                     |           |
| 2     | 1.1                | 61.7       | 1.429 ± .05              |                  | -0.0028            |             |                                     |           |
| 3     | 2.2                | 3.089      | 1.510 ± .33              |                  | -0.036             |             |                                     |           |
| 4     | 3.3                | 2.83       | 1.384 ± .32              |                  | -0.073             |             |                                     |           |
| 5     | 4.4                | 3.21       | 1.43 ± .29               |                  | -0.173             |             |                                     |           |
| 6     | 5.5                | 4.50       | 1.47 ± .17 (0.69)        |                  | -0.128             |             |                                     |           |
| 7     | 6.6                | 3.49       | 1.58 ± .22 0.90          |                  | -0.111             |             |                                     |           |
| 8     | 7.7                | 1.67       | 1.63 ± .52 0.98          |                  | -0.266             |             |                                     |           |
| 9     | 8.8                | 1.02       | 1.68 ± .77 1.06          |                  | -0.408             | 27.3 ↔ 24.3 | $5.5 \times 10^{-12} 1.4 \times 10$ |           |
| 10    | 9.9                | 1.55       | 2.04 ± .59 1.57          |                  | -0.414             | 24.5        | $5.6 \times 10^{-12} 1.4 \times 10$ |           |
| 11    | 11.0               | 2.34       | 1.88 ± .41 1.36          |                  | -0.383             | 28.7        | $7.7 \times 10^{-12} 1.9 \times 10$ |           |
| 12    | 12.1               | 2.93       | 1.99 ± .36 1.51          |                  | -0.415             |             |                                     |           |
| 13    | 13.2               | 3.32       | 2.39 ± .35 2.01          |                  | -0.256             | 28.4        | $7.5 \times 10^{-12} 1.9 \times 10$ |           |
| 14    | 14.3               | 3.13       | 2.31 ± .30 1.91          |                  | -0.359             |             |                                     |           |
| 15    | 15.4               | 2.51       | 2.42 ± .37 2.04          |                  | -0.265             |             |                                     |           |
| 16    | 16.5               | 1.84       | 3.14 ± .66 2.86          |                  | -0.217             | 21.7        | $4.4 \times 10^{-12} 1.1 \times 10$ |           |
| 17    | 17.6               | 2.69       | 3.30                     | 3.03             | -0.087             |             |                                     |           |
| 18    | 18.7               | 3.19       | 3.58                     | 3.34             | -0.335             |             |                                     |           |
| 19    | 19.8               | 3.39       | 3.37                     | 3.11             | -0.202             |             |                                     |           |
| 20    | 20.9               | 3.13       | 3.16                     | 2.88             | -0.489             |             |                                     |           |
| 21    | 22.0               | 3.42       | 3.10                     | 2.81             | -0.402             |             |                                     |           |
| 22    | 23.1               | 3.83       | 3.32                     | 3.05             | -0.295             |             |                                     |           |
| 23    | 24.2               | 3.94       | 3.20                     | 2.92             | -0.168             |             |                                     |           |
| 24    | 25.3               | 3.98       | 3.08                     | 2.79             | -0.189             |             |                                     |           |
| 25    | 26.4               | 4.03       | 3.05                     | 2.76             | -0.290             | 27.4        | $7.0 \times 10^{-12} 1.8 \times 10$ |           |
| 26    | 27.5               | 3.31       | 3.16                     | 2.88             | -0.328             |             |                                     |           |
| 27    | 28.6               | 2.55       | 3.39                     | 3.13             | -0.484             |             |                                     |           |
| 28    | 29.7               | 2.30       | 4.27                     | 4.07             | -0.234             |             |                                     |           |
| 29    | 30.8               | 2.72       | 3.82                     | 3.59             | -0.259             |             |                                     |           |
| 30    | 31.9               | 3.18       | 3.69                     | 3.48             | -0.250             | 24.0        | $5.4 \times 10^{-12} 1.4 \times 10$ |           |
| 31    | 33.0               | 2.70       | 3.66                     | 3.42             | -0.304             |             |                                     |           |
| 32    | 34.1               | 1.93       | 4.30                     | 4.10             | -0.263             |             |                                     |           |
| 33    | 35.2               | 2.10       | 4.09                     | 3.88             | -0.190             |             |                                     |           |
| 34    | 36.3               | 1.97       | 4.41                     | 4.21             | -0.504             |             |                                     |           |
| 35    | 37.4               | 1.67       | 4.09                     | 3.88             | -0.533             |             |                                     |           |
| 36    | 38.5               | 1.10       | 5.02                     | 4.85             | -0.998             | 16.1        | $2.4 \times 10^{-12} 6.1 \times 10$ |           |
| 37    | 39.6               | 0.978      | 4.23                     | 4.03             | -0.977             |             |                                     |           |
| 38    | 40.7               | 1.16       | 4.63                     | 4.44             | -0.839             |             |                                     |           |
| 39    | 41.8               | 1.15       | 5.35                     | 5.19             | -0.701             |             |                                     |           |
| 40    | 42.9               | 1.11       | 4.75                     | 4.57             | -0.625             |             |                                     |           |
| 41    | 44.0               | 1.02       | 4.53                     | 4.34             | -0.922             |             |                                     |           |
| 42    | 45.1               | 1.38       | 5.03                     | 4.86             | -0.478             |             |                                     |           |
| 43    | 46.2               | 1.64       | 4.79                     | 4.61             | -0.408             |             |                                     |           |
| 44    | 47.3               | 1.65       | 5.05                     | 4.83             | -0.361             |             |                                     |           |
| 45    | 48.4               | 2.56       | 4.56                     | 4.37             | -0.276             |             |                                     |           |
| 46    | 49.5               | 3.05       | 4.41                     | 4.21             | -0.224             | 22.4        | $4.7 \times 10^{-12} 1.2 \times 10$ |           |
| 47    | 50.6               | 2.34       | 4.84                     | 4.66             | -0.148             |             |                                     |           |
| 48    | 51.7               | 1.75       | 5.39                     | 5.23             | -0.229             |             |                                     |           |
| 49    | 52.8               | 1.29       | 5.46                     | 5.30             | -0.372             |             |                                     |           |
| 50    | 53.9               | 1.18       | 4.95                     | 4.75             | -0.697             |             |                                     |           |

1" 3

|    | $\theta''$ | Imax  | $\bar{I}''$ | $\bar{I}_0$ | $\Delta''$ | $B_{eq}$ | $U_{min}$            | $nT$            |
|----|------------|-------|-------------|-------------|------------|----------|----------------------|-----------------|
| 51 | 55.0       | 1.04  | 4.61        | 4.42        | -0.821     |          |                      |                 |
| 52 | 56.1       | 1.07  | 4.03        | 3.81        | -0.823     |          |                      |                 |
| 53 | 57.2       | 0.889 | 4.11        | 3.90        | -0.724     | 16.1     | $2.4 \times 10^{-2}$ | $6.1 \times 10$ |
| 54 | 58.3       | 0.387 | 2.01        |             | +0.841     |          |                      |                 |
| 55 | 59.4       | 0.709 | 6.95        | 6.83        | -0.541     |          |                      |                 |
| 56 | 60.5       | 1.01  | 5.47        | 5.31        | -0.614     |          |                      |                 |
| 57 | 61.6       | 0.936 | 5.10        | 4.93        | -0.815     |          |                      |                 |
| 58 | 62.7       | 1.01  | 4.88        | 4.70        | -0.978     |          |                      |                 |
| 59 | 63.8       | 1.14  | 4.50        | 4.31        | -1.043     | 16.8     | $2.6 \times 10^{-2}$ | $6.7 \times 10$ |
| 60 | 64.9       | 1.13  | 5.19        | 5.02        | -0.914     |          |                      |                 |
| 61 | 66.0       | 0.904 | 7.02        | 6.90        | -1.067     |          |                      |                 |
| 62 | 67.1       | 0.860 | 4.95        | 4.78        | -1.700     |          |                      |                 |
| 63 | 68.2       | 1.086 | 5.44        | 5.28        | -1.247     |          |                      |                 |
| 64 | 69.3       | 1.29  | 5.30        | 5.14        | -1.459     |          |                      |                 |
| 65 | 70.4       | 1.56  | 4.85        | 4.67        | -1.436     |          |                      |                 |
| 66 | 71.5       | 1.67  | 4.41        | 4.21        | -1.247     | 18.9     | $3.3 \times 10^{-2}$ | $8.4 \times 10$ |
| 67 | 72.6       | 1.61  | 4.17        | 3.96        | -1.385     |          |                      |                 |
| 68 | 73.7       | 1.61  | 4.43        | 4.23        | -1.429     |          |                      |                 |
| 69 | 74.8       | 1.51  | 4.26        | 4.06        | -0.875     |          |                      |                 |
| 70 | 75.9       | 1.52  | 4.02        | 3.80        | -1.148     |          |                      |                 |
| 71 | 77.0       | 1.55  | 4.22        | 4.01        | -1.380     |          |                      |                 |
| 72 | 78.1       | 1.20  | 6.65        | 6.52        | -1.173     |          |                      |                 |
| 73 | 79.2       | 1.14  | 5.64        | 5.49        | -1.316     |          |                      |                 |
| 74 | 80.3       | 1.09  | 5.38        | 5.22        | -0.753     | 15.7     | $2.3 \times 10^{-2}$ | $5.8 \times 10$ |
| 75 | 81.4       | 0.981 | 5.70        | 5.55        | -0.876     |          |                      |                 |
| 76 | 82.5       | 1.28  | 5.55        | 5.40        | -0.869     |          |                      |                 |
| 77 | 83.6       | 1.71  | 4.70        | 4.52        | -0.990     |          |                      |                 |
| 78 | 84.7       | 2.04  | 4.78        | 4.60        | -0.784     | 19.5     | $3.5 \times 10^{-2}$ | $9.0 \times 10$ |
| 79 | 85.8       | 1.85  | 4.93        | 4.76        | -0.398     |          |                      |                 |
| 80 | 86.9       | 1.86  | 4.56        | 4.37        | -0.370     |          |                      |                 |
| 81 | 88.0       | 1.65  | 5.00        | 4.83        | -0.352     |          |                      |                 |
| 82 | 89.1       | 1.32  | 5.19        | 5.02        | -0.474     |          |                      |                 |
| 83 | 90.2       | 1.18  | 5.36        | 5.20        | -1.110     |          |                      |                 |
| 84 | 91.3       | 1.18  | 5.68        | 5.53        | -1.644     |          |                      |                 |
| 85 | 92.4       | 1.02  | 6.07        | 5.93        | -1.513     |          |                      |                 |
| 86 | 93.5       | 0.945 | 6.01        | 5.87        | -1.574     |          |                      |                 |
| 87 | 94.6       | 0.860 | 7.19        | 7.07        | -0.662     | 13.5     | $1.7 \times 10^{-2}$ | $4.3 \times 10$ |
| 88 | 95.7       | 0.904 | 7.22        | 7.10        | -1.041     |          |                      |                 |
| 89 | 96.8       | 1.036 | 6.13        | 5.99        | -0.605     |          |                      |                 |
| 90 | 97.9       | 1.050 | 6.21        | 6.07        | -0.056     |          |                      |                 |
| 91 | 99.0       | 1.291 | 5.99        | 5.85        | -0.097     |          |                      |                 |
| 92 | 100.1      | 1.49  | 5.67        | 5.52        | -0.122     | 16.9     | $2.7 \times 10^{-2}$ | $6.8 \times 10$ |
| 93 | 101.2      | 1.37  | 5.23        | 5.07        | -0.321     |          |                      |                 |
| 94 | 102.3      | 1.04  | 6.16        | 6.02        | -0.777     |          |                      |                 |
| 95 | 103.4      | 0.905 | 6.72        | 6.59        | -0.656     |          |                      |                 |
| 96 | 104.5      | 0.913 | 6.78        | 6.65        | -0.299     |          |                      |                 |
| 97 | 105.6      | 0.790 | 7.33        | 7.21        | -0.411     |          |                      |                 |
| 98 | 106.7      | 0.888 | 6.57        | 6.44        | -0.396     |          |                      |                 |
| 99 | 107.8      | 0.980 | 6.11        | 5.97        | -0.201     |          |                      |                 |

NGC6251 1662 MHz 2" 11 record.

| SLICE | $\theta''$ | $I_{max}^{maj}$ | $\bar{I}''$ | $\bar{I}_0$ | $\frac{\partial \bar{I}}{\partial I_{1.3}}$ | $\Delta''$ |  |  |  |
|-------|------------|-----------------|-------------|-------------|---------------------------------------------|------------|--|--|--|
| 1     | 0          | 432             |             |             |                                             |            |  |  |  |
| 2     | 1.5        | 111.5           |             |             |                                             | -0.0072    |  |  |  |
| 3     | 3          | 6.74            |             |             |                                             | -0.0423    |  |  |  |
| 4     | 4.5        | 5.87            | 2.24        | 0.75        | 2.23                                        | -0.138     |  |  |  |
| 5     | 6          | 6.78            | 2.31        | 0.94        | 2.57                                        | -0.132     |  |  |  |
| 6     | 7.5        | 3.75            | 2.38        | 1.10        | 1.42                                        | -0.208     |  |  |  |
| 7     | 9          | 2.29            | 2.47        | 1.28        | 0.87                                        | -0.358     |  |  |  |
| 8     | 10.5       | 3.66            | 2.61        | 1.36        | 1.39                                        | -0.401     |  |  |  |
| 9     | 12         | 5.54            | 2.75        | 1.76        | 2.10                                        | -0.370     |  |  |  |
| 10    | 13.5       | 6.33            | 3.07        | 2.23        | 2.40                                        | -0.290     |  |  |  |
| 11    | 15         | 5.68            | 2.99        | 2.12        | 2.16                                        | -0.296     |  |  |  |
| 12    | 16.5       | 4.72            | 3.46        | 2.74        | 1.79                                        | -0.175     |  |  |  |
| 13    | 18         | 6.64            | 3.89        | 3.27        | 2.52                                        | -0.239     |  |  |  |
| 14    | 19.5       | 7.72            | 3.83        | 3.20        | 2.93                                        | -0.320     |  |  |  |
| 15    | 21         | 7.38            | 3.60        | 2.92        | 2.80                                        | -0.398     |  |  |  |
| 16    | 22.5       | 8.17            | 3.64        | 2.97        | 3.10                                        | -0.324     |  |  |  |
| 17    | 24         | 8.84            | 3.63        | 3.02        | 3.36                                        | -0.227     |  |  |  |
| 18    | 25.5       | 9.03            | 3.62        | 2.94        | 3.43                                        | -0.200     |  |  |  |
| 19    | 27         | 8.21            | 3.56        | 2.87        | 3.12                                        | -0.311     |  |  |  |
| 20    | 28.5       | 6.12            | 3.89        | 3.27        | 2.32                                        | -0.438     |  |  |  |
| 21    | 30         | 6.03            | 4.17        | 3.60        | 2.29                                        | -0.342     |  |  |  |
| 22    | 31.5       | 7.09            | 3.94        | 3.33        | 2.63                                        | -0.247     |  |  |  |
| 23    | 33         | 6.11            | 4.15        | 3.57        | 2.32                                        | -0.250     |  |  |  |
| 24    | 34.5       | 4.92            | 4.49        | 3.96        | 1.87                                        | -0.303     |  |  |  |
| 25    | 36         | 4.70            | 4.47        | 3.94        | 1.78                                        | -0.428     |  |  |  |
| 26    | 37.5       | 3.69            | 4.68        | 4.18        | 1.40                                        | -0.560     |  |  |  |
| 27    | 39         | 2.48            | 5.44        | 5.01        | 0.94                                        | -0.874     |  |  |  |
| 28    | 40.5       | 2.60            | 5.21        | 4.76        | 0.99                                        | -0.848     |  |  |  |
| 29    | 42         | 2.82            | 5.30        | 4.86        | 1.07                                        | -0.631     |  |  |  |
| 30    | 43.5       | 2.66            | 5.08        | 4.62        | 1.01                                        | -0.665     |  |  |  |
| 31    | 45         | 3.21            | 5.41        | 4.98        | 1.22                                        | -0.648     |  |  |  |
| 32    | 46.5       | 4.10            | 5.19        | 4.74        | 1.56                                        | -0.469     |  |  |  |
| 33    | 48         | 5.36            | 4.97        | 4.50        | 2.03                                        | -0.306     |  |  |  |
| 34    | 49.5       | 6.52            | 4.86        | 4.38        | 2.48                                        | -0.083     |  |  |  |
| 35    | 51.0       | 5.27            | 5.14        | 4.69        | 2.00                                        | -0.194     |  |  |  |
| 36    | 52.5       | 3.55            | 5.68        | 5.27        | 1.35                                        | -0.291     |  |  |  |
| 37    | 54         | 2.71            | 5.57        | 5.15        | 1.03                                        | -0.624     |  |  |  |
| 38    | 55.5       | 2.56            | 4.52        | (4.00)      |                                             | -0.958     |  |  |  |
| 39    | 57         | 2.17            | 4.64        | (4.13)      |                                             | -0.841     |  |  |  |
| 40    | 58.5       | 1.78            | 6.24        | 5.87        | 0.68                                        | -0.611     |  |  |  |
| 41    | 60         | 2.22            | 5.80        | 5.40        | 0.84                                        | -0.485     |  |  |  |
| 42    | 61.5       | 2.30            | 5.45        | 5.02        | 0.87                                        | -0.782     |  |  |  |
| 43    | 63         | 2.53            | 4.86        | 4.38        | 0.96                                        | -0.985     |  |  |  |
| 44    | 64.5       | 2.16            | 5.12        | 4.67        | 1.05                                        | -1.045     |  |  |  |
| 45    | 66         | 2.27            | 6.54        | (6.19)      | 0.86                                        | -1.124     |  |  |  |
| 46    | 67.5       | 2.27            | 5.76        | 5.36        | 0.86                                        | -1.426     |  |  |  |
| 47    | 69.0       | 3.26            | 5.26        | 4.82        | 1.24                                        | -1.503     |  |  |  |
| 48    | 70.5       | 3.81            | 5.13        | (5.68)      | 1.45                                        | -1.383     |  |  |  |
| 49    | 72         | 3.91            | 5.04        | 4.58        | 1.48                                        | -1.339     |  |  |  |
| 50    | 73.5       | 3.18            | 4.98        | 4.51        | 1.44                                        | -1.373     |  |  |  |

2.11 cont'd

| #  | $\Theta''$ | $I_{max}$ | $\Theta'$ | $\Theta_0$ | $I_{1.3}^{equv}$ | $\Delta''$ | $B_{eq}$ | $U_{min}$             | $nT$              |
|----|------------|-----------|-----------|------------|------------------|------------|----------|-----------------------|-------------------|
| S1 | 75         | 3.73      | 4.48      | 3.95       | 1.42             | -1.082     |          |                       |                   |
| S2 | 76.5       | 3.68      | 4.60      | 4.09       | 1.40             | -1.216     |          |                       |                   |
| S3 | 78         | 3.17      | 6.32      | 5.95       | 1.20             | -1.228     |          |                       |                   |
| S4 | 79.5       | 2.88      | 6.07      | 5.69       | 1.09             | -1.104     |          |                       |                   |
| S5 | 81         | 2.59      | 5.67      | 5.26       | 0.98             | -0.942     |          |                       |                   |
| S6 | 82.5       | 3.24      | 5.62      | 5.21       | 1.23             | -1.034     |          |                       |                   |
| S7 | 84         | 4.31      | 5.20      | 4.75       | 1.64             | -0.840     |          |                       |                   |
| S8 | 85.5       | 4.66      | 5.15      | 4.70       | 1.77             | -0.517     |          |                       |                   |
| S9 | 87         | 4.26      | 5.20      | 4.75       | 1.62             | -0.381     |          |                       |                   |
| S0 | 88.5       | 3.59      | 5.56      | 5.14       | 1.36             | -0.409     |          |                       |                   |
| S1 | 90         | 2.84      | 6.01      | 5.63       | 1.08             | -0.818     |          |                       |                   |
| S2 | 91.5       | 2.75      | 6.39      | 6.03       | 1.04             | -1.383     | 14.9     | $2.1 \times 10^{-12}$ | $5.2 \times 10^3$ |
| S3 | 93         | 2.58      | 6.39      | 6.03       | 0.98             | -1.334     |          |                       |                   |
| S4 | 94.5       | 2.21      | 7.16      | 6.81       | 0.84             | -0.941     |          |                       |                   |
| S5 | 96         | 2.46      | 7.31      | 7.50       | 0.93             | -0.882     |          |                       |                   |
| S6 | 97.5       | 2.75      | 6.89      | 6.56       | 1.04             | -0.482     |          |                       |                   |
| S7 | 99         | 3.24      | 6.26      | 5.89       | 1.23             | -0.173     |          |                       |                   |
| S8 | 100.5      | 3.52      | 5.95      | 5.56       | 1.34             | -0.277     |          |                       |                   |
| S9 | 102        | 2.77      | 6.22      | 5.85       | 1.05             | -0.614     |          |                       |                   |
| S0 | 103.5      | 2.44      | 7.05      | 6.72       | 0.93             | -0.511     |          |                       |                   |
| S1 | 105        | 2.33      | 7.29      | 6.98       | 0.88             | -0.379     | 13.6     | $1.7 \times 10^{-12}$ | $4.4 \times 10^3$ |
| S2 | 106.5      | 2.33      | 7.08      | 6.76       | 0.88             | -0.447     |          |                       |                   |
| S3 | 108        | 2.68      | 6.40      | 6.04       | 1.02             | -0.432     |          |                       |                   |
| S4 | 109.5      | 3.16      | 6.23      | 5.86       | 1.20             | -0.538     |          |                       |                   |
| S5 | 111        | 2.81      | 7.06      | 6.74       | 1.07             | -0.687     |          |                       |                   |
| S6 | 112.5      | 2.38      | 7.72      | 7.43       | 0.90             | -0.521     | 13.5     | $1.7 \times 10^{-12}$ | $4.3 \times 10^3$ |
| S7 | 114        | 2.58      | 7.66      | 7.36       | 0.98             | +0.211     |          |                       |                   |
| S8 | 115.5      | 2.11      | 8.64      | 8.38       | 0.80             | +0.301     | 12.6     |                       |                   |
| S9 | 117        | 1.73      | 9.56      | 9.32       | 0.66             | 0.464      | 11.5     | $1.2 \times 10^{-12}$ | $3.1 \times 10^3$ |
| S0 | 118.5      | 1.61      | 8.71      | 8.45       | 0.61             | 0.397      |          |                       |                   |
| S1 | 120.0      | 1.53      | 8.86      | 8.61       | 0.58             | 0.508      |          |                       |                   |
| S2 | 121.5      | 1.33      | 9.64      | 9.41       | 0.50             | 0.420      | 10.6     | $1.1 \times 10^{-12}$ | $2.7 \times 10^3$ |
| S3 | 123        | 1.13      | 13.29     | (13.12)    | 0.43             | 0.307      |          |                       |                   |
| S4 | 124.5      | 1.17      | 15.07     | (14.92)    |                  | 0.474      |          |                       |                   |
| S5 | 126        | 1.13      | 11.81     | 11.62      | 0.43             | 0.144      | 10.0     | $9.4 \times 10^{-13}$ | $2.4 \times 10^3$ |
| S6 | 127.5      | 0.962     | 12.67     | 12.49      | 0.37             | 0.167      | 8.95     | $7.5 \times 10^{-13}$ | $1.9 \times 10^3$ |
| S7 | 129        | 0.85      | 14.38     | 14.22      | 0.32             | -0.346     | 8.33     | $6.5 \times 10^{-13}$ | $1.6 \times 10^3$ |
| S8 | 130.5      | 0.987     | 14.24     | 14.08      | 0.37             | 0.177      |          |                       |                   |
| S9 | 132        | 0.985     | 13.17     | 13.0       | 0.37             | 0.678      | 8.91     | $7.4 \times 10^{-15}$ |                   |
| S0 | 133.5      | 0.901     | 12.83     | 12.66      | 0.34             | 0.702      |          |                       |                   |

NGC 6251

"4.39 Resolution"

1662 MHz

Cellsize = 3.5'' S

| SUC# | $\Theta(^{\circ})$ | $I_{max}^{mJy}$ | $\Phi(^{\circ})$ | <del><math>I_{1.3}^{eqn}</math></del> | $I_{1.3}^{eqn}$ | $\Delta(^{\circ})$ | $I_{1.3}^{eqn}$ | Beg<br>magans | $U_{min}$<br>$J\text{ m}^{-2}$ | $nT$<br>$m^3\text{ K}$ |
|------|--------------------|-----------------|------------------|---------------------------------------|-----------------|--------------------|-----------------|---------------|--------------------------------|------------------------|
| 1    | 0                  | 43.19           | 4.75             | 0.50                                  | 1.81            | -0.00078           |                 |               |                                |                        |
| 2    | 3.5                | 85.1            | 4.78             | 0.53                                  | 1.89            | -0.0199            |                 |               |                                |                        |
| 3    | 7.0                | 10.0            | 4.84             | 0.53                                  | 2.04            | -0.189             |                 |               |                                |                        |
| 4    | 10.5               | 9.07            | 5.08             | 1.60                                  | 2.56            | -0.363             |                 |               |                                |                        |
| 5    | 14                 | 14.1            | 5.36             | 0.48                                  | 3.08            | -0.320             |                 |               |                                |                        |
| 6    | 17.5               | 17.4            | 5.57             | 2.90                                  | 3.43            | -0.241             |                 |               |                                |                        |
| 7    | 21                 | 22.1            | 5.51             | 2.70                                  | 3.33            | -0.320             |                 |               |                                |                        |
| 8    | 24.5               | 24.3            | 5.53             | 2.83                                  | 3.36            | -0.270             |                 |               |                                |                        |
| 9    | 28                 | 20.5            | 5.62             | 2.99                                  | 3.51            | -0.316             |                 |               |                                |                        |
| 10   | 31.5               | 18.9            | 5.83             | 3.57                                  | 3.84            | -0.243             |                 |               |                                |                        |
| 11   | 35                 | 15.2            | 6.09             | 3.81                                  | 4.22            | -0.346             |                 |               |                                |                        |
| 12   | 38.5               | 10.1            | 6.34             | 4.20                                  | 4.57            | -0.604             |                 |               |                                |                        |
| 13   | 42                 | 8.66            | 6.54             | 4.50                                  | 4.85            | -0.697             |                 |               |                                |                        |
| 14   | 45.5               | 12.02           | 6.60             | 4.58                                  | 4.93            | -0.532             |                 |               |                                |                        |
| 15   | 49                 | 18.1            | 6.45             | 4.33                                  | 4.73            | -0.252             | 1.59            |               |                                |                        |
| 16   | 52.5               | 13.1            | 6.75             | 4.80                                  | 5.13            | -0.314             | 1.15            |               |                                |                        |
| 17   | 56                 | 7.53            | 6.42             | 4.32                                  | 4.68            | -0.705             | 0.660           |               |                                |                        |
| 18   | 59.5               | 6.63            | 6.90             | 5.00                                  | 5.32            | -0.568             | 0.581           |               |                                |                        |
| 19   | 63                 | 7.72            | 6.41             | 4.30                                  | 4.67            | -0.921             | 0.677           |               |                                |                        |
| 20   | 66.5               | 8.03            | 6.78             | 4.84                                  | 5.17            | -1.205             | 0.709           |               |                                |                        |
| 21   | 70                 | 11.10           | 6.46             | 4.38                                  | 4.74            | -1.369             | 0.973           |               |                                |                        |
| 22   | 73.5               | 11.8            | 6.26             | 4.08                                  | 4.46            | -1.211             | 1.04            |               |                                |                        |
| 23   | 77                 | 10.9            | 6.59             | 4.37                                  | 4.91            | -1.133             | 0.956           |               |                                |                        |
| 24   | 80.5               | 10.0            | 7.07             | 5.24                                  | 5.54            | -0.953             | 0.877           |               |                                |                        |
| 25   | 84                 | 13.2            | 6.59             | 4.57                                  | 4.91            | -0.732             | 1.16            |               |                                |                        |
| 26   | 87.5               | 13.1            | 6.80             | 4.87                                  | 5.19            | -0.481             | 1.15            |               |                                |                        |
| 27   | 91                 | 9.58            | 7.45             | 5.74                                  | 6.02            | -0.977             | 0.840           |               |                                |                        |
| 28   | 94.5               | 8.51            | 7.71             | 6.07                                  | 6.34            | -0.988             | 0.746           |               |                                |                        |
| 29   | 98                 | 10.2            | 7.48             | 5.78                                  | 6.06            | -0.434             | 0.894           |               |                                |                        |
| 30   | 101.5              | 10.3            | 7.31             | 5.86                                  | 5.84            | -0.390             | 0.903           |               |                                |                        |
| 31   | 105                | 8.50            | 7.90             | 6.31                                  | 6.57            | -0.477             | 0.745           |               |                                |                        |
| 32   | 108.5              | 9.61            | 7.47             | 5.77                                  | 6.04            | -0.464             | 0.843           |               |                                |                        |
| 33   | 112                | 9.42            | 8.04             | 6.49                                  | 6.74            | -0.405             | 0.826           |               |                                |                        |
| 34   | 115.5              | 7.75            | 8.65             | 7.23                                  | 7.45            | +0.224             | 0.680           |               |                                |                        |
| 35   | 119                | 5.79            | 9.27             | 6.90                                  | 8.16            | 0.344              | 0.508           |               |                                |                        |
| 36   | 122.5              | 4.82            | 10.03            | 8.83                                  | 9.02            | 0.118              | 0.423           |               |                                |                        |
| 37   | 126                | 4.05            | 10.36            | 8.21                                  | 9.38            | 0.110              | 0.355           |               |                                |                        |
| 38   | 129.5              | 3.39            | 10.54            | 9.41                                  | 9.58            | 0.343              | 0.297           |               |                                |                        |
| 39   | 133                | 3.38            | 10.65            | 9.53                                  | 9.7             | 0.946              | 0.296           |               |                                |                        |
| 40   | 136.5              | 3.71            | 11.77            | 10.77                                 | 10.92           | 0.927              | 0.325           |               |                                |                        |
| 41   | 140                | 5.05            | 9.83             | 8.61                                  | 8.8             | -0.0006            | 0.443           |               |                                |                        |
| 42   | 143.5              | 5.07            | 9.12             | 7.79                                  | 7.99            | -0.159             | 0.445           | 9.07          | $7.68 \times 10^{-13}$         | $1.94 \times 10^{42}$  |
| 43   | 147                | 3.96            | 10.29            | 9.18                                  | 9.31            | -0.103             | 0.347           |               |                                |                        |
| 44   | 150.5              | 3.14            | 10.85            | 9.75                                  | 9.92            | +0.191             | 0.275           |               |                                |                        |
| 45   | 154                | 2.62            | 10.64            | 9.52                                  | 9.69            | +0.193             | 0.230           |               |                                |                        |
| 46   | 157.5              | 2.68            | 11.38            | 10.54                                 | 10.50           | +0.338             | 0.235           |               |                                |                        |
| 47   | 161                | 2.67            | 12.25            | 11.29                                 | 11.44           | +0.339             | 0.234           |               |                                |                        |
| 48   | 164.5              | 2.18            | 14.32            | 13.81                                 | 13.63           | +0.150             | 0.191           | 6.52          | $2.58 \times 10^{-13}$         | $652 \times 10^{42}$   |
| 49   | 168                | 2.201           | 13.76            | 12.91                                 | 12.14           | -0.459             | 0.198           |               |                                |                        |
| 50   | 171.5              | 2.11            | 11.97            | 10.94                                 | 11.09           | +0.131             | 0.229           |               |                                |                        |

NGC 6251

4.39 resol.

1662 MHz  
Cell ~~3.5~~ 3.5

| SLICE | $\Theta$ | $I_{max}^{eq}$ | $\bar{\Theta} (")$ | $\bar{\Theta}_o$ | $\Delta (")$ | $I_{1.3}^{eque}$ | $B_{eq}$ | $4mm$                  | $nT$                  |
|-------|----------|----------------|--------------------|------------------|--------------|------------------|----------|------------------------|-----------------------|
| 51    | 175      | 3.68           | 12.54              | 11.75            | +0.679       | 0.323            |          |                        |                       |
| 52    | 178.5    | 5.18           | 11.27              | 10.38            | +0.693       | 0.454            |          |                        |                       |
| 53    | 182      | 6.82           | 10.64              | 9.69             | -0.296       | 0.572            |          |                        |                       |
| 54    | 185.5    | 6.91           | 9.89               | 8.86             | -0.585       | 0.606            |          |                        |                       |
| 55    | 189      | 7.82           | 9.66               | 8.60             | -1.162       | 0.686            |          |                        |                       |
| 56    | 192.5    | 9.90           | 9.26               | 8.15             | -1.114       | 0.868            | 10.9     | $1.10 \times 10^{-12}$ | $2.78 \cdot 10^{10}$  |
| 57    | 196      | 8.10           | 10.48              | 9.51             | -0.983       | 0.710            |          |                        |                       |
| 58    | 199.5    | 6.25           | 11.30              | 10.4             | -0.414       | 0.548            | 8.28     | $6.41 \times 10^{-13}$ | $1.62 \cdot 10^{10}$  |
| 59    | 203      | 7.70           | 12.37              | 11.56            | +0.941       | 0.675            |          |                        |                       |
| 60    | 206.5    | 16.0           | 10.29              | 9.31             | +1.114       | 1.403            |          |                        |                       |
| 61    | 210      | 17.5           | 10.12              | 9.12             | 0.959        | 1.54             | 12.0     | $1.34 \times 10^{-12}$ | $3.39 \cdot 10^{10}$  |
| 62    | 213.5    | 11.4           | 11.29              | 10.40            | -0.304       | 1.150            |          |                        |                       |
| 63    | 217      | 6.82           | 13.0               | 12.23            | -1.583       | 0.598            | 7.74     | $5.60 \times 10^{-13}$ | $1.42 \times 10^{10}$ |
| 64    | 220.5    | 7.64           | 13.6               | 12.87            | -1.529       | 0.670            |          |                        |                       |
| 65    | 224      | 11.20          | 13.3               | 12.6             | -1.801       | 0.982            |          |                        |                       |
| 66    | 227.5    | 13.9           | 13.4               | 12.7             | -1.632       | 1.219            |          |                        |                       |
| 67    | 231      | 14.1           | 12.7               | 11.9             | -1.791       | 1.24             | 9.67     | $8.74 \times 10^{-13}$ | $2.21 \times 10^{10}$ |
| 68    | 234.5    | 10.4           | 13.3               | 12.6             | -1.561       | 0.912            |          |                        |                       |
| 69    | 238      | 8.17           | 16.4               | 15.8             | +0.247       | 0.716            | 7.04     | $4.63 \times 10^{-13}$ | $1.17 \times 10^{10}$ |
| 70    | 241.5    | 10.85          | 15.1               | 14.4             | +0.999       | 0.981            |          |                        |                       |
| 71    | 245      | 10.65          | 14.7               | 14.0             | 1.404        | 0.934            |          |                        |                       |
| 72    | 248.5    | 9.68           | 15.0               | 14.3             | 2.397        | 0.849            |          |                        |                       |
| 73    | 252      | 8.83           | 14.7               | 14.0             | 3.787        | 0.774            | 10.7     | $1.08 \times 10^{-12}$ | $2.7 \times 10^{10}$  |
| 74    | 255.5    | 7.23           | 14.3               | 13.6             | 4.580        | 0.634            |          |                        |                       |
| 75    | 259      | 5.15           | 16.0               | 15.4             | 5.800        | 0.450            |          |                        |                       |
| 76    | 262.5    | 3.24           | 18.1               | 17.6             | 7.555        | 0.284            | 5.08     | $2.41 \times 10^{-13}$ | $6.1 \times 10^9$     |
| 77    | 266      | 2.56           | 17.9               | 17.4             | 9.350        | 0.224            |          |                        |                       |
| 78    | 269.5    | 1.82           | 19.2               | 18.7             | 10.22        | 0.160            |          |                        |                       |
| 79    | 273      | 1.31           | 21.9               | 21.5             | 11.05        | 0.115            |          |                        |                       |
| 80    | 276.5    | 1.27           | 19.3               | 18.8             | 11.58        | 0.111            | 3.74     | $1.31 \times 10^{-13}$ | $3.31 \times 10^9$    |

# HBC turbulence - NEC6251

NATIONAL  
42-384  
Manufactured U.S.A.

| $\Theta$ | $\Phi$   | $ d\bar{\Phi}/d\theta $ | $\langle d\bar{\Phi}/d\theta \rangle$ | $\langle \cdot \rangle^3$ | $v_j$  | $v_j/\bar{\Phi}$  | $(v_j/\bar{\Phi})^2$ | $\langle \cdot \rangle^2 (\cdot)^2$ | $\log_{10}$ |
|----------|----------|-------------------------|---------------------------------------|---------------------------|--------|-------------------|----------------------|-------------------------------------|-------------|
| 1.6      | (0.12)   |                         |                                       |                           |        |                   |                      |                                     |             |
| 2.0      | (0.1278) | 0.020                   | 0.020                                 | $8 \times 10^{-6}$        | 1.33   | $1.04 \cdot 10^1$ | $1.08 \cdot 10^2$    | $8.66 \cdot 10^{-4}$                | -3.06       |
| 3        | (0.1826) | 0.055                   | 0.055                                 | $1.66 \cdot 10^{-4}$      | 1.80   | 9.59              | 97.2                 | $1.61 \cdot 10^0$                   | -1.79       |
| 4        | (0.257)  | 0.074                   | 0.074                                 | $4.05 \cdot 10^{-4}$      | 2.05   | 7.98              | 63.6                 | $2.58 \cdot 10^2$                   | -1.59       |
| 5        | (0.35)   | 0.093                   | 0.093                                 | $8.04 \cdot 10^{-4}$      | 2.17   | 6.20              | 38.4                 | $3.09 \cdot 10^2$                   | -1.51       |
| 6        | (0.50)   | 0.15                    | 0.15                                  | $3.38 \cdot 10^{-3}$      | 2.26   | 4.52              | 20.4                 | $6.91 \cdot 10^{-2}$                | -1.16       |
| 7        | (0.85)   | 0.35                    | 0.35                                  | $4.19 \cdot 10^{-2}$      | 2.32   | 2.73              | 7.45                 | $3.20 \cdot 10^1$                   | -0.49       |
| 9        | 1.35     | 0.25                    | 0.20                                  | $8 \cdot 10^{-3}$         | 2.38   | 1.76              | 3.11                 | $2.49 \cdot 10^2$                   | -1.60       |
| 11       | 1.55     | 0.10                    | 0.175                                 | $5.36 \cdot 10^{-3}$      | 2.43   | 1.57              | 2.46                 | $1.32 \cdot 10^2$                   | -1.88       |
| 15       | 2.15     | 0.15                    | 0.15                                  | $3.38 \cdot 10^{-3}$      | 2.475  | 1.15              | 1.33                 | $4.48 \cdot 10^3$                   | -2.35       |
| 17       | 2.60     | 0.225                   | 0.15                                  | $3.38 \cdot 10^{-3}$      | 2.487  | 0.957             | 0.915                | $3.09 \cdot 10^3$                   | -2.51       |
| 29       | 2.85     | 0.125                   | 0.13                                  | $2.20 \cdot 10^{-3}$      | 2.49   | 0.874             | 0.763                | $1.68 \cdot 10^3$                   | -2.78       |
| 21       | 2.95     | 0.050                   | 0.08                                  | $5.12 \cdot 10^{-4}$      | 2.493  | 0.845             | 0.714                | $3.66 \cdot 10^4$                   | -3.44       |
| 23       | 3.00     | 0.025                   | 0.03                                  | $2.70 \cdot 10^{-5}$      | 2.4935 | 0.831             | 0.691                | $1.87 \cdot 10^5$                   | -4.73       |
| 25       | 3.00     | 0.050                   | 0.0                                   | 0.00                      |        |                   |                      |                                     |             |
| 27       | 3.05     | 0.025                   | 0.025                                 | $1.56 \cdot 10^{-5}$      | 2.485  | 0.815             | 0.664                | $1.04 \cdot 10^5$                   | -4.99       |
| 29       | 3.25     | 0.100                   | 0.07                                  | $3.43 \cdot 10^{-4}$      | 2.48   | 0.763             | 0.582                | $2.00 \cdot 10^4$                   | -3.70       |
| 31       | 3.40     | 0.075                   | 0.09                                  | $7.29 \cdot 10^{-4}$      | 2.475  | 0.728             | 0.530                | $3.86 \cdot 10^4$                   | -3.41       |
| 33       | 3.65     | 0.125                   | 0.125                                 | $1.95 \cdot 10^{-3}$      | 2.472  | 0.677             | 0.459                | $8.94 \cdot 10^4$                   | -3.05       |
| 35       | 3.90     | 0.125                   | 0.125                                 | $1.95 \cdot 10^{-3}$      | 2.473  | 0.634             | 0.402                | $7.84 \cdot 10^4$                   | -3.11       |
| 37       | 4.10     | 0.100                   | 0.110                                 | $1.33 \cdot 10^{-3}$      | 2.478  | 0.604             | 0.365                | $4.86 \cdot 10^4$                   | -3.31       |
| 39       | 4.35     | 0.125                   | 0.110                                 | $1.33 \cdot 10^{-3}$      | 2.486  | 0.572             | 0.327                | $4.34 \cdot 10^4$                   | -3.36       |
| 41       | 4.50     | 0.075                   | 0.08                                  | $5.12 \cdot 10^{-4}$      | 2.49   | 0.553             | 0.306                | $1.57 \cdot 10^4$                   | -3.81       |
| 43       | 4.60     | 0.050                   | 0.06                                  | $2.16 \cdot 10^{-4}$      | 2.50   | 0.544             | 0.295                | $6.38 \cdot 10^5$                   | -4.20       |
| 45       | 4.70     | 0.050                   | 0.05                                  | $1.25 \cdot 10^{-4}$      | 2.51   | 0.534             | 0.285                | $3.56 \cdot 10^5$                   | -4.45       |
| 47       | 4.80     | 0.050                   | 0.05                                  | $1.25 \cdot 10^{-4}$      | 2.515  | 0.524             | 0.275                | $3.43 \cdot 10^5$                   | -4.46       |
| 49       | 4.85     | 0.025                   | 0.025                                 | $1.56 \cdot 10^{-5}$      | 2.52   | 0.520             | 0.270                | $4.21 \cdot 10^6$                   | -5.38       |
| 51       | 4.90     | 0.025                   | 0.025                                 | $1.56 \cdot 10^{-5}$      | 2.523  | 0.515             | 0.265                | $4.14 \cdot 10^6$                   | -5.38       |
| 53       | 4.95     | 0.025                   | 0.025                                 | $1.56 \cdot 10^{-5}$      | 2.527  | 0.511             | 0.261                | $4.07 \cdot 10^6$                   | -5.39       |
| 55       | 4.97     | 0.010                   | 0.010                                 | $1.00 \cdot 10^{-6}$      | 2.531  | 0.509             | 0.259                | $2.59 \cdot 10^7$                   | -6.59       |
| 57       | 4.99     | 0.010                   | 0.010                                 | $1.00 \cdot 10^{-6}$      | 2.531  | 0.507             | 0.257                | $2.57 \cdot 10^7$                   | -6.59       |
| 59       | 5.00     | 0.005                   | 0.005                                 | $1.26 \cdot 10^{-7}$      | 2.532  | 0.506             | 0.256                | $3.21 \cdot 10^8$                   | -7.49       |
| 80       | 5.05     | 0.0024                  | 0.0024                                | $1.38 \cdot 10^{-8}$      | 2.53   | 0.501             | 0.251                | $3.46 \cdot 10^9$                   | -8.46       |
| 82       | 5.1      | 0.025                   | 0.025                                 | $1.56 \cdot 10^{-5}$      | 2.53   | 0.496             | 0.246                | $3.84 \cdot 10^6$                   | -5.42       |
| 84       | 5.2      | 0.050                   | 0.050                                 | $1.25 \cdot 10^{-4}$      | 2.532  | 0.487             | 0.237                | $2.96 \cdot 10^5$                   | -4.53       |
| 86       | 5.32     | 0.060                   | 0.060                                 | $2.16 \cdot 10^{-4}$      | 2.534  | 0.476             | 0.227                | $4.90 \cdot 10^5$                   | -4.31       |
| 88       | 5.53     | 0.105                   | 0.105                                 | $1.16 \cdot 10^{-3}$      | 2.535  | 0.458             | 0.210                | $2.44 \cdot 10^4$                   | -3.61       |
| 90       | 5.74     | 0.105                   | 0.105                                 | $1.16 \cdot 10^{-3}$      | 2.537  | 0.442             | 0.195                | $2.27 \cdot 10^4$                   | -3.64       |
| 92       | 6.0      | 0.13                    | 0.13                                  | $2.20 \cdot 10^{-3}$      | 2.54   | 0.423             | 0.179                | $3.94 \cdot 10^4$                   | -3.40       |
| 94       | 6.4      | 0.20                    | 0.20                                  | $3.60 \cdot 10^{-3}$      | 2.542  | 0.397             | 0.158                | $1.26 \cdot 10^3$                   | -2.90       |
| 96       | 6.6      | 0.10                    | 0.10                                  | $1.00 \cdot 10^{-3}$      | 2.545  | 0.386             | 0.149                | $1.47 \cdot 10^4$                   | -3.83       |
| 98       | 6.4      | 0.10                    | 0.10                                  | $1.00 \cdot 10^{-3}$      | 2.548  | 0.398             | 0.159                | $1.59 \cdot 10^4$                   | -3.50       |
| 100      | 6.1      | 0.15                    | 0.125                                 | $3.45 \cdot 10^{-3}$      | 2.551  | 0.418             | 0.175                | $3.41 \cdot 10^4$                   | -3.28       |
| 102      | 5.9      | 0.15                    | 0.15                                  | $3.38 \cdot 10^{-3}$      | 2.553  | 0.440             | 0.194                | $6.54 \cdot 10^4$                   | -3.18       |
| 104      | 6.25     | 0.225                   | 0.225                                 | $1.14 \cdot 10^{-2}$      | 2.555  | 0.409             | 0.167                | $1.91 \cdot 10^3$                   | -2.72       |
| 106      | 6.8      | 0.275                   | 0.275                                 | $2.08 \cdot 10^{-2}$      | 2.557  | 0.376             | 0.141                | $2.99 \cdot 10^3$                   | -2.53       |
| 108      | 6.3      | 0.25                    | 0.27                                  | $1.56 \cdot 10^{-2}$      | 2.559  | 0.406             | 0.165                | $2.57 \cdot 10^3$                   | -2.59       |
| 110      | 5.8/6.3  | 0.25                    | 0.26                                  | $1.56 \cdot 10^{-2}$      | 2.561  | 0.416             | 0.173                | $2.70 \cdot 10^3$                   | -2.57       |
| 112      | 6.8      | 0.25                    | 0.25                                  | $1.56 \cdot 10^{-2}$      | 2.563  | 0.376             | 0.142                | $2.21 \cdot 10^3$                   | -2.65       |
| 114      | 7.25     | 0.225                   | 0.25                                  | $1.14 \cdot 10^{-2}$      | 2.565  | 0.354             | 0.125                | $1.43 \cdot 10^3$                   | -2.85       |
| 116      | 7.9      | 0.325                   | 0.30                                  | $3.43 \cdot 10^{-2}$      | 2.567  | 0.325             | 0.106                | $3.62 \cdot 10^3$                   | -2.44       |

HBC Turbulence - NGCG 251 cont'd.

| $\Theta$ | $\Phi$ | $ d\phi/d\theta $ | $\langle \cdot \rangle$ | $\langle \cdot \rangle^2$ | $v_j$ | $(v_j/\Phi)$ | $(\cdot)^2$ | $\langle \cdot \rangle^3 (\cdot)^2$ | $10\tau_{10}$ |
|----------|--------|-------------------|-------------------------|---------------------------|-------|--------------|-------------|-------------------------------------|---------------|
| 118      | 8.4    | 0.25              | 0.25                    | $1.56 \cdot 10^{-2}$      | 2.568 | 0.306        | 0.093       | $1.46 \cdot 10^{-3}$                | -2.84         |
| 120      | 8.7    | 0.15              | 0.16                    | $4.10 \cdot 10^{-3}$      | 2.568 | 0.295        | 0.087       | $3.57 \cdot 10^{-4}$                | -3.45         |
| 122      | 8.95   | 0.125             | 0.14                    | $2.74 \cdot 10^{-3}$      | 2.569 |              | 0.082       | $2.25 \cdot 10^{-4}$                | -3.65         |
| 124      | 9.2    | 0.125             | 0.125                   | $1.95 \cdot 10^{-3}$      | 2.57  | 0.279        | 0.078       | $1.52 \cdot 10^{-4}$                | -3.82         |
| 126      | 9.4    | 0.10              | 0.10                    | $1 \cdot 10^{-3}$         | 2.571 | 0.274        | 0.075       | $7.48 \cdot 10^{-5}$                | -4.13         |
| 128      | 9.55   | 0.05              | 0.08                    | $5.12 \cdot 10^{-4}$      | 2.571 |              | 0.073       | $3.75 \cdot 10^{-5}$                | -4.43         |
| 130      | 9.65   | 0.075             | 0.06                    | $2.16 \cdot 10^{-4}$      | 2.572 | 0.267        | 0.071       | $1.53 \cdot 10^{-5}$                | -4.81         |
| 132      | 9.70   | 0.025             | 0.03                    | $2.70 \cdot 10^{-5}$      | 2.573 |              | 0.070       | $1.90 \cdot 10^{-6}$                | -5.72         |
| 134      | 9.70   | 0.000             | 0.00                    | —                         | 2.574 |              |             |                                     |               |
| 136      | 9.60   | 0.05              | 0.05                    | $1.25 \cdot 10^{-4}$      | 2.575 | 0.268        | 0.072       | $8.99 \cdot 10^{-6}$                | -5.05         |
| 138      | 9.4    | 0.1               | 0.1                     | $10^{-3}$                 | 2.576 | 0.274        | 0.075       | $7.51 \cdot 10^{-5}$                | -4.12         |
| 140      | 8.9    | 0.25              | 0.25                    | $1.56 \cdot 10^{-2}$      | 6     | 0.289        | 0.084       | $1.31 \times 10^{-3}$               | -2.88         |
| 142      | 8.4    | 0.25              | 0.25                    | $1.56 \cdot 10^{-2}$      | 7     |              |             | $1.47 \cdot 10^{-3}$                | -2.83         |
| 144      | 8.3    | 0.05              | 0.1                     | $10^{-3}$                 | 7     |              |             | $3.1 \cdot 10^{-4}$                 | -3.51         |
| 146      | 8.45   | 0.075             | 0.06                    | $2.16 \cdot 10^{-4}$      | 8     |              | 0.093       | $2.01 \cdot 10^{-5}$                | -4.70         |
| 148      | 8.75   | 0.15              | 0.15                    | $3.38 \cdot 10^{-3}$      | 2.578 |              |             | $2.93 \cdot 10^{-4}$                | -3.53         |
| 150      | 8.15   | 0.2               | 0.18                    | $5.83 \cdot 10^{-3}$      | 8     |              |             | $4.63 \cdot 10^{-4}$                | -3.33         |
| 152      | 9.5    | 0.175             | 0.18                    | $5.83 \cdot 10^{-3}$      | 9     |              |             | $4.58 \cdot 10^{-4}$                | -3.37         |
| 154      | 9.9    | 0.2               | 0.2                     | $8 \cdot 10^{-3}$         | 2.579 |              |             | $5.43 \cdot 10^{-4}$                | -3.27         |
| 156      | 10.2   | 0.15              | 0.15                    | $3.38 \cdot 10^{-3}$      | 9     |              |             | $2.16 \cdot 10^{-4}$                | -3.67         |
| 158      | 10.8   | 0.3               | 0.15                    | $3.38 \cdot 10^{-3}$      | 80    |              |             | $1.93 \cdot 10^{-4}$                | -3.71         |
| 160      | 10.95  | 0.075             | 0.15                    | $3.38 \cdot 10^{-3}$      | 0     |              |             | $1.88 \cdot 10^{-4}$                | -3.73         |
| 162      | 11.3   | 0.175             | 0.18                    | $5.83 \cdot 10^{-3}$      | 0     |              |             | $3.04 \cdot 10^{-4}$                | -3.52         |
| 164      | 11.55  | 0.125             | 0.18                    | $5.83 \cdot 10^{-3}$      | 2.580 |              |             | $2.91 \cdot 10^{-4}$                | -3.54         |
| 166      | 11.85  | 0.15              | 0.15                    | $3.38 \cdot 10^{-3}$      | 0     |              |             | $1.60 \cdot 10^{-4}$                | -3.80         |
| 168      | 12.1   | 0.125             | 0.15                    | $2.20 \cdot 10^{-3}$      | 1     |              |             | $1.00 \cdot 10^{-4}$                | -4.00         |
| 170      | 12.25  | 0.075             | 0.1                     | $10^{-3}$                 | 1     |              |             | $4.44 \cdot 10^{-5}$                | -4.35         |
| 172      | 12.1   | 0.075             | 0.08                    | $5.12 \cdot 10^{-4}$      | 1     |              |             | $2.33 \cdot 10^{-5}$                | -4.63         |
| 174      | 11.8   | 0.15              | 0.15                    | $3.38 \cdot 10^{-3}$      | 1     |              |             | $1.62 \cdot 10^{-4}$                | -3.79         |
| 176      | 11.2   | 0.3               | 0.3                     | $2.70 \cdot 10^{-2}$      | 1     |              |             | $1.43 \cdot 10^{-3}$                | -2.84         |
| 178      | 10.6   | 0.3               | 0.3                     | $2.7 \cdot 10^{-2}$       | 2     |              |             | $6.58 \cdot 10^{-3}$                | -2.18         |
| 180      | 10.2   | 0.2               | 0.25                    | $1.56 \cdot 10^{-2}$      | 2     |              |             | $1.0 \cdot 10^{-3}$                 | -3.00         |
| 182      | 9.8    | 0.2               | 0.2                     | $8 \cdot 10^{-3}$         | 2     |              |             | $5.55 \cdot 10^{-4}$                | -3.26         |
| 184      | 9.45   | 0.175             | 0.18                    | $5.83 \cdot 10^{-3}$      | 2.582 |              |             | $4.35 \cdot 10^{-4}$                | -3.36         |
| 186      | 9.1    | 0.175             | 0.16                    | $4.10 \cdot 10^{-3}$      | 2     |              |             | $3.30 \cdot 10^{-4}$                | -3.48         |
| 188      | 8.8    | 0.15              | 0.15                    | $3.38 \cdot 10^{-3}$      | 2     |              |             | $2.92 \cdot 10^{-4}$                | -3.54         |
| 190      | 8.45   | 0.175             | 0.13                    | $2.20 \cdot 10^{-3}$      | 3     |              |             | $2.06 \cdot 10^{-4}$                | -3.60         |
| 192      | 8.3    | 0.075             | 0.08                    | $5.12 \cdot 10^{-4}$      | 3     |              |             | $4.96 \cdot 10^{-5}$                | -4.30         |
| 194      | 8.4    | 0.05              | 0.05                    | $1.25 \cdot 10^{-4}$      | 3     |              |             | $1.18 \cdot 10^{-5}$                | -4.93         |
| 196      | 8.8    | 0.2               | 0.1                     | $10^{-3}$                 | 2.583 |              |             | $8.62 \cdot 10^{-5}$                | -4.06         |
| 198      | 9.6    | 0.4               | 0.3                     | $2.7 \cdot 10^{-2}$       | 3     |              |             | $1.95 \cdot 10^{-3}$                | -2.71         |
| 200      | 10.4   | 0.4               | 0.4                     | $6.4 \cdot 10^{-2}$       | 3     |              |             | $3.95 \cdot 10^{-3}$                | -2.40         |
| 202      | 11.8   | 0.7               | 0.5                     | $1.25 \cdot 10^{-1}$      | 4     |              |             | $5.99 \cdot 10^{-3}$                | -2.22         |
| 204      | 11.8   | 0.0               | 0.21                    | $6.4 \cdot 10^{-2}$       | 4     |              |             | $3.07 \cdot 10^{-3}$                | -2.51         |
| 206      | 11.5   | 0.15              | 0.2                     | $2.7 \cdot 10^{-2}$       | 4     |              |             | $1.36 \cdot 10^{-3}$                | -2.87         |
| 208      | 9.6    | 0.45              | 0.2                     | $8 \cdot 10^{-3}$         | 2.584 |              |             | $5.80 \cdot 10^{-4}$                | -3.24         |
| 210      | 9.2    | 0.2               | 0.2                     | $8 \cdot 10^{-3}$         | 4     |              |             | $6.31 \cdot 10^{-4}$                | -3.20         |
| 212      | 9.4    | 0.1               | 0.15                    | $3.38 \cdot 10^{-3}$      | 5     |              |             | $2.56 \cdot 10^{-4}$                | -3.59         |
| 214      | 10.15  | 0.375             | 0.18                    | $5.83 \cdot 10^{-3}$      | 5     |              |             | $3.78 \cdot 10^{-4}$                | -3.42         |
| 216      | 10.5   | 0.175             | 0.18                    | $5.83 \cdot 10^{-3}$      | 6     |              |             | $3.59 \cdot 10^{-4}$                | -3.45         |
| 218      | 11.3   | 0.1               | 0.1                     | $10^{-3}$                 | 2.586 |              |             | $3.24 \cdot 10^{-5}$                | -4.28         |

Fits to NGC6251 1480MHz 1S"

| H   | $\Delta$ | S   | $\Delta$ |
|-----|----------|-----|----------|
| 12  | - 0.016  | 324 | +13.95   |
| 24  | - 0.333  | 336 | +15.53   |
| 36  | - 0.381  | 348 | +20.10   |
| 48  | - 0.544  | 360 | +18.00   |
| 60  | - 0.672  | 372 | +17.62   |
| 72  | - 1.299  | 384 | +16.39   |
| 84  | - 1.193  | 396 | +17.32   |
| 96  | - 0.911  | 408 | +24.10   |
| 108 | - 0.611  | 420 | +29.22   |
| 120 | - 0.304  | 432 | +37.19   |
| 132 | + 1.304  | 444 | +44.61   |
| 144 | + 1.966  | 456 | +52.36   |
| 156 | + 2.103  | 468 | + ???    |
| 168 | + 4.021  | 480 | +67.79 ? |
| 180 | - 0.055  | 492 | +61.73   |
| 192 | - 0.810  | 504 | +124.6   |
| 204 | - 0.397  |     |          |
| 216 | - 0.031  |     |          |
| 228 | - 1.487  |     |          |
| 240 | - 0.869  |     |          |
| 252 | + 1.719  |     |          |
| 264 | + 4.951  |     |          |
| 276 | + 9.080  |     |          |
| 288 | + 11.32  |     |          |
| 300 | + 11.93  |     |          |
| 312 | + 14.60  |     |          |

— Burbidge GR, Odeh SL  
ApJ, 178, 583 (1972)

— Leksi RT and Roeder RC  
JRASC, 66, 1111 (1972)

## Power Spectra of NGC6251 oscillations.

Theoretical deflection probability for random noise:

$$\Pi(P > P_0) \Rightarrow 1 - \{1 - \exp(-P_0)\}^n$$

Where  $n(k_1 < k < k_2) = \left(\frac{k_2 - k_1}{2\pi}\right)(\theta_2 - \theta_1)$

$\theta_1 \rightarrow \theta_2$  data range  
 $k_1 \rightarrow k_2$  spect range

$$\sim 0.5 \times 98 \sim 50 \text{ in our case.}$$

So  $\Pi \sim 1 - \exp(-50 \exp(-P_0))$

|                             |                                      |
|-----------------------------|--------------------------------------|
| $\sim 0.29$ for $P_0 = 5$   | , i.e. $\sim 15$ occurrences / spec. |
| $\sim 0.045$ for $P_0 = 7$  | $\sim 2$ occurrences / spec          |
| $\sim 0.002$ for $P_0 = 10$ | $\sim 1$ occurrence / spec.          |

i.e.  $P(>5)$  is  $\sim 7 \times P(>7)$  (we saw  $\sim 5 \times$ )

$P > 10$  is  $\sim \frac{1}{20} P(>7)$  SAFE

For the shorter deflections,  $n \sim 0.5 \times 40 \sim 20$

$$\Pi \sim 1 - \exp(-20 \exp(-P_0))$$

|                             |
|-----------------------------|
| $\sim 0.13$ for $P_0 = 5$   |
| $\sim 0.02$ for $P_0 = 7$   |
| $\sim 0.001$ for $P_0 = 10$ |

1 occurrence in 50 spectra

$P = 10 \times$  mean is fairly safe, and easy to read.

Compute significances piece by piece though, they vary.

Turn semi

|      |    |
|------|----|
| 143" | 9" |
| 31"  |    |
| 7.5" |    |
| 12"  |    |

Hence:-

Average angle data  $20'' < \theta < 100''$

|         |        |                             |                                 |                      |                |                  |
|---------|--------|-----------------------------|---------------------------------|----------------------|----------------|------------------|
| Peak or | 0.0234 | $\cdot 4199 \times 10^{-6}$ | is $\sim 7.9 \times \text{bgd}$ | $\pi = .008$         | 1 in 6 spectra | $\times 85$      |
|         | 0.112  | $\cdot 8139 \times 10^{-7}$ | is $\sim 8.1 \times -$          | .006                 | 8              | $\times 17$      |
|         | 0.172  | $\cdot 477 \times 10^{-7}$  | 12.2 $\times$                   |                      | 490 spectra    | $\checkmark 11$  |
|         | 0.287  | $\cdot 223 \times 10^{-7}$  | 16 $\times$                     | $2.3 \times 10^{-6}$ | 2115 spectra   | $\checkmark 7.0$ |
|         | 0.359  | $\cdot 122 \times 10^{-7}$  | 28 $\times$ -                   |                      | Uncomplete     | $\checkmark 5.6$ |

$\Rightarrow$  SIGN peaks  $11.6, 7.0, 5.6$

Average angle data  $0'' < \theta < 100''$

|       |                        |                            |                 |                   |
|-------|------------------------|----------------------------|-----------------|-------------------|
| 0.292 | $10 \times \text{bgd}$ | $\pi = 9.3 \times 10^{-4}$ | 1 in 52 spectra | $\checkmark 6.85$ |
| 0.359 | 11 $\times$            | $3.4 \times 10^{-4}$       | 1 in 143 sp-    | $\checkmark 5.6$  |

1".3 angle data  $0'' < \theta < 100''$

|       |                          |                            |                 |                  |
|-------|--------------------------|----------------------------|-----------------|------------------|
| 0.190 | $10.4 \times \text{bgd}$ | $\pi = 1.5 \times 10^{-3}$ | 1 in 14 spectra | $\checkmark 5.8$ |
|-------|--------------------------|----------------------------|-----------------|------------------|

1".3 deflection data  $0'' < \theta < 100''$

|       |                         |                            |                  |                  |
|-------|-------------------------|----------------------------|------------------|------------------|
| 0.190 | $9.3 \times \text{bgd}$ | $\pi = 4.5 \times 10^{-3}$ | 1 in 4.6 spectra | $\checkmark 5.8$ |
|-------|-------------------------|----------------------------|------------------|------------------|

2".1 angle data  $0'' < \theta < 134''$

|        |                          |                            |                 |                  |
|--------|--------------------------|----------------------------|-----------------|------------------|
| 0.0885 | $7.7 \times \text{bgd}$  | $\pi = 2.0 \times 10^{-2}$ | 1 in 1.2        | $\times 16.9$    |
| 0.166  | $11.5 \times \text{bgd}$ | $\pi = 4.5 \times 10^{-4}$ | 1 in 51 spectra | $\checkmark 9.0$ |
| 0.260  | 11.1 $\times$            | $\pi = 6.6 \times 10^{-4}$ | 1 in 34         | $\checkmark 5.8$ |

2".1 angle data  $15'' < \theta < 134''$

|       |                          |                            |           |                  |
|-------|--------------------------|----------------------------|-----------|------------------|
| 0.166 | $16.2 \times \text{bgd}$ | $\pi = 3.5 \times 10^{-6}$ | 1 in 7170 | $\checkmark 9.0$ |
| 0.260 | 23 $\times$              | $\pi = -$                  | -         | $\checkmark 5.6$ |
| 0.31  | 10 $\times$              |                            | 1 in 14   | $\checkmark 4.8$ |

4" angle zero  $125^\circ < \theta < 276^\circ$

0.148

0.102

0.274

0.372

$10.3 \times \text{bgnd}$   
 $10.2 \times$

$$\Pi = 7.4 \times 10^{-4}$$
$$8.2 \times 10^{-2}$$

1 in 62 spectra  
1 in 56

23".6

34".3

12".7

9".4

4".4 angle delta  $'80'' < \theta < 276''$

No significant peaks

15" angle zero  $210'' < \theta < 440''$

0.029

0.086

0.141

sidelobes at 230" bad aliasing

413"

140"

85"

2".1 angle zero  $30'' < \theta < 100''$

0.115

0.163

$10.2 \times \text{bgnd}$   
 $9.1 \times \text{bgnd}$

0.001  
0.504

1 in 26 spectra  
1 in 9 spectra

13".0

9".2

1".3 angle zero  $30'' < \theta < 100''$

0.190

0.083

0.140

$26.3 \times \text{bgnd}$

$5.8 \times \text{bgnd}$

5.2 ×

small

$\infty$

5".8

13".3

15" angle zero  $0'' < \theta < 456''$

0.0781

$7.5 \times \text{bgnd}$

$$\Pi = 0.010$$

1 in 5.1 spectra

153".6

22 July 1982

CH fir to NGC6251

$$z_s = 0.6864 \text{ (kpc)}$$

$$\alpha = 1.0$$

$$n = 4.15$$

Core infreqsion

$$1.6 \times 10^5 \text{ cells}$$

$$p_s = 4 \times 10^8 \text{ cm}^{-3} \text{ K}$$

$$n_e T \sim 4 \times 10^8$$

$$n_e = 10, T = 4 \times 10^7 \quad n = 20, T = 2 \times 10^7 \quad n = 40, T = 10^7$$

$$R_{\max} = 1 \text{ M} \quad 8.83 \times 10^8 \quad 1.77 \times 10^9 \quad 3.53 \times 10^9 \text{ M}$$

$$L_x \quad 6.39 \times 10^{43} \quad 2.13 \times 10^{44} \quad 5.10 \times 10^{44} \frac{\text{erg}}{\text{sec}}$$

$$2 \quad 1.44 \times 10^9 \quad 2.88 \times 10^9 \quad 5.77 \times 10^9$$

$$6.98 \times 10^{43} \quad 2.33 \times 10^{44} \quad 5.57 \times 10^{44}$$

$$10 \quad 1.85 \times 10^9 \quad 3.70 \times 10^9 \quad 7.48 \times 10^9$$

$$6.99 \times 10^{43} \quad 2.33 \times 10^{44} \quad 5.58 \times 10^{44}$$

$$20 \quad 1.89 \times 10^9 \quad 3.78 \times 10^9 \quad 7.58 \times 10^9$$

$$6.99 \times 10^{43} \quad 2.33 \times 10^{44} \quad 5.58 \times 10^{44}$$

Conclude: At  $T = 2 \times 10^7 \text{ K}$

Core has  $L_x \sim 2.3 \times 10^{44} \text{ erg/sec}$

90% within 1 kpc of center

22 July 1982

CH fit to NGC6251

$$z_s = 16.73 \text{ kpc}$$

$$\alpha = 1.0$$

$$m = 2.60$$

halo integration

$1.6 \times 10^5$  cells.

$$\phi_s = 4 \times 10^5 \text{ cm}^{-3} \text{ K} \quad (\text{halo})$$

$$n_e = 10^{-2} \quad T = 4 \times 10^7 \quad n_e = 2 \times 10^{-2} \quad T = 2 \times 10^7 \quad n_e = 4 \times 10^{-2} \quad T = 10^8$$

|                        |       |                       |                       |                       |
|------------------------|-------|-----------------------|-----------------------|-----------------------|
| $R_{\text{max}} = 100$ | M     | $8.41 \times 10^{10}$ | $1.68 \times 10^{11}$ | $3.36 \times 10^{11}$ |
|                        | $L_x$ | $1.97 \times 10^{42}$ | $6.56 \times 10^{42}$ | $1.57 \times 10^{43}$ |

|     |       |                       |                       |                       |
|-----|-------|-----------------------|-----------------------|-----------------------|
| 200 | M     | $1.38 \times 10^{11}$ | $2.76 \times 10^{11}$ | $5.52 \times 10^{11}$ |
|     | $L_x$ | $2.01 \times 10^{42}$ | $6.68 \times 10^{42}$ | $1.60 \times 10^{43}$ |

|     |       |                       |                       |                       |
|-----|-------|-----------------------|-----------------------|-----------------------|
| 300 | M     | $1.77 \times 10^{11}$ | $3.55 \times 10^{11}$ | $7.09 \times 10^{11}$ |
|     | $L_x$ | $2.01 \times 10^{42}$ | $6.70 \times 10^{42}$ | $1.60 \times 10^{43}$ |

|    |       |                       |                       |                       |
|----|-------|-----------------------|-----------------------|-----------------------|
| 50 | M     | $4.39 \times 10^{10}$ | $8.78 \times 10^{10}$ | $1.76 \times 10^{11}$ |
|    | $L_x$ | $1.81 \times 10^{42}$ | $6.02 \times 10^{42}$ | $1.44 \times 10^{43}$ |

Conclude: At  $T = 2 \times 10^7 \text{ K}$

Halo has  $L_x \sim 6.7 \times 10^{42} \text{ erg/sec}$

90% within 50 kpc of center

N.B. Divide L's by 1.352  
M's by 1.163

NGC6251  
 $\log\text{-}\log L_{\text{min}}(\odot)$   
 $(\equiv nT)$

$nT \text{ cm}^{-3} \text{ K}$

46 7400

K+E LOGARITHMIC 3 X 3 CYCLES  
 KEUFFEL & ESSER CO. MADE IN U.S.A.

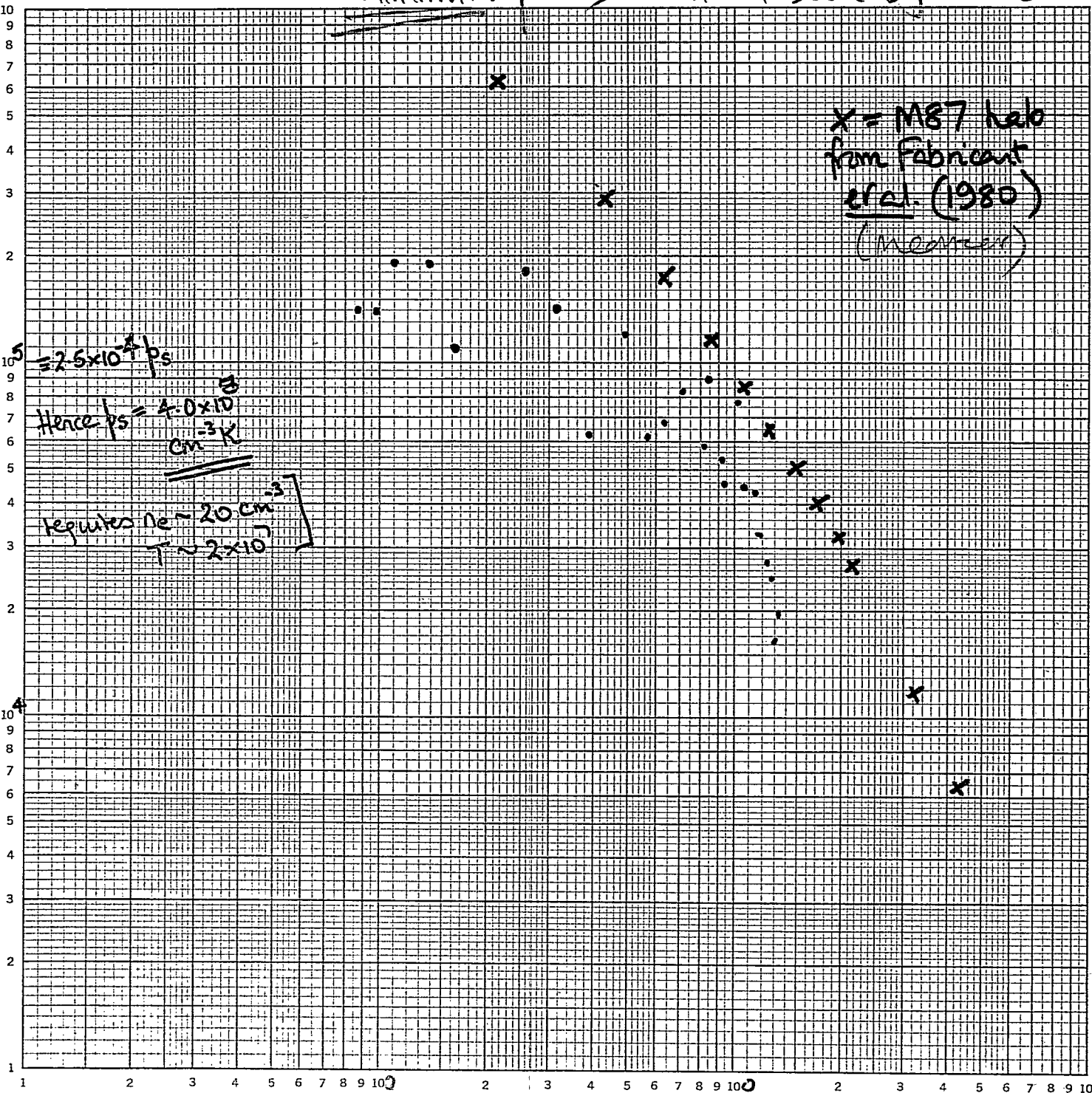
Minimum  $\rightarrow$  Mult  $nT$  Scale by 0.86

$x = 1A87$  halo  
 from Fabre et al. (1980)  
 (mean)

$$= 2.5 \times 10^4 \text{ ps}$$

$$\text{Hence } \rho_s = 4.0 \times 10^{13} \text{ cm}^{-3} \text{ K}$$

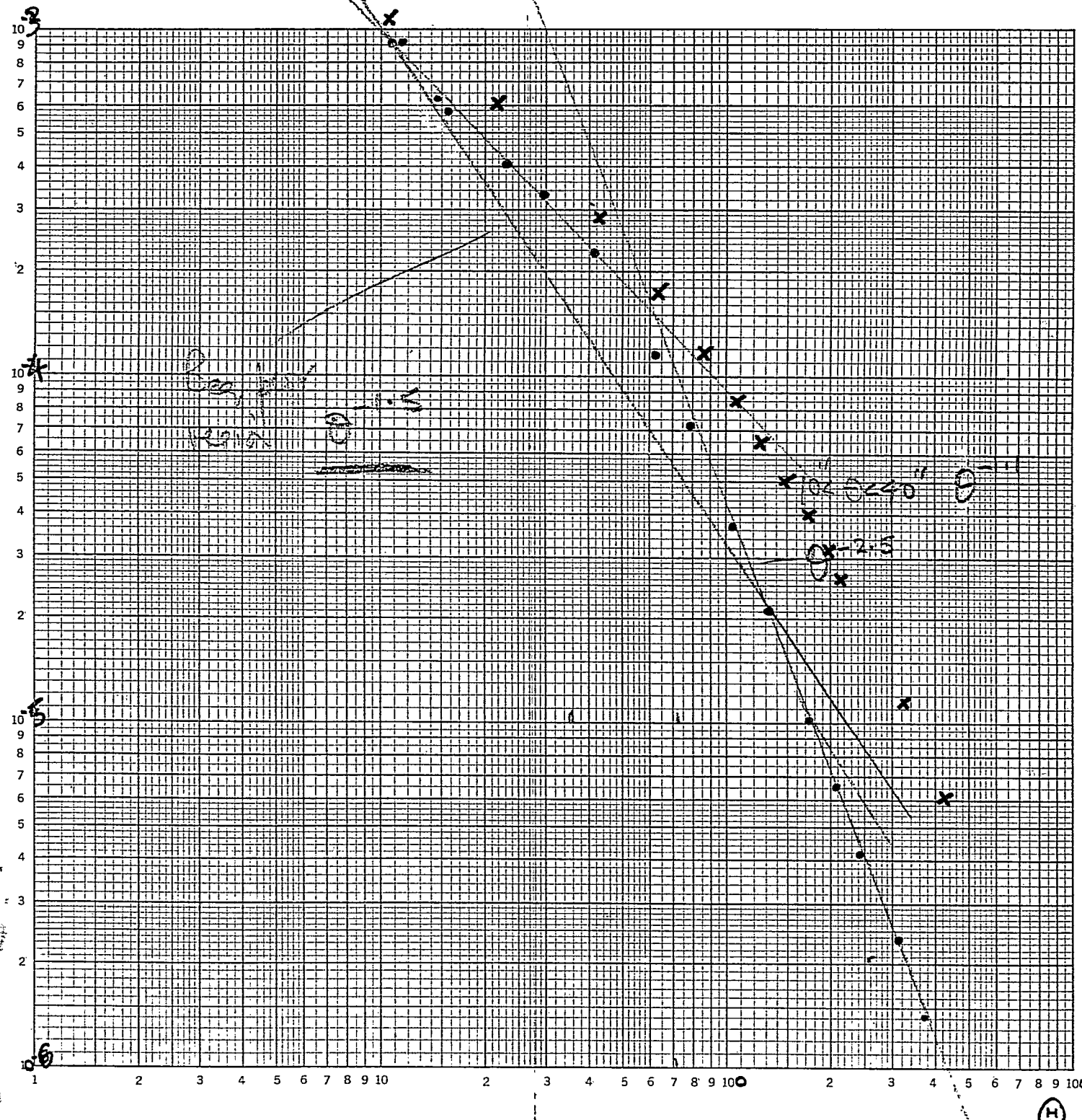
$$\text{Requires } n_e \sim 20 \text{ cm}^{-3} \\ \sim 2 \times 10^5$$



NGC 6251  
log-log  $\rho_e(z)$

46 7400

K E LOGARITHMIC 3 X 3 CYCLES  
KEUFFEL & ESSER CO. MADE IN U.S.A.



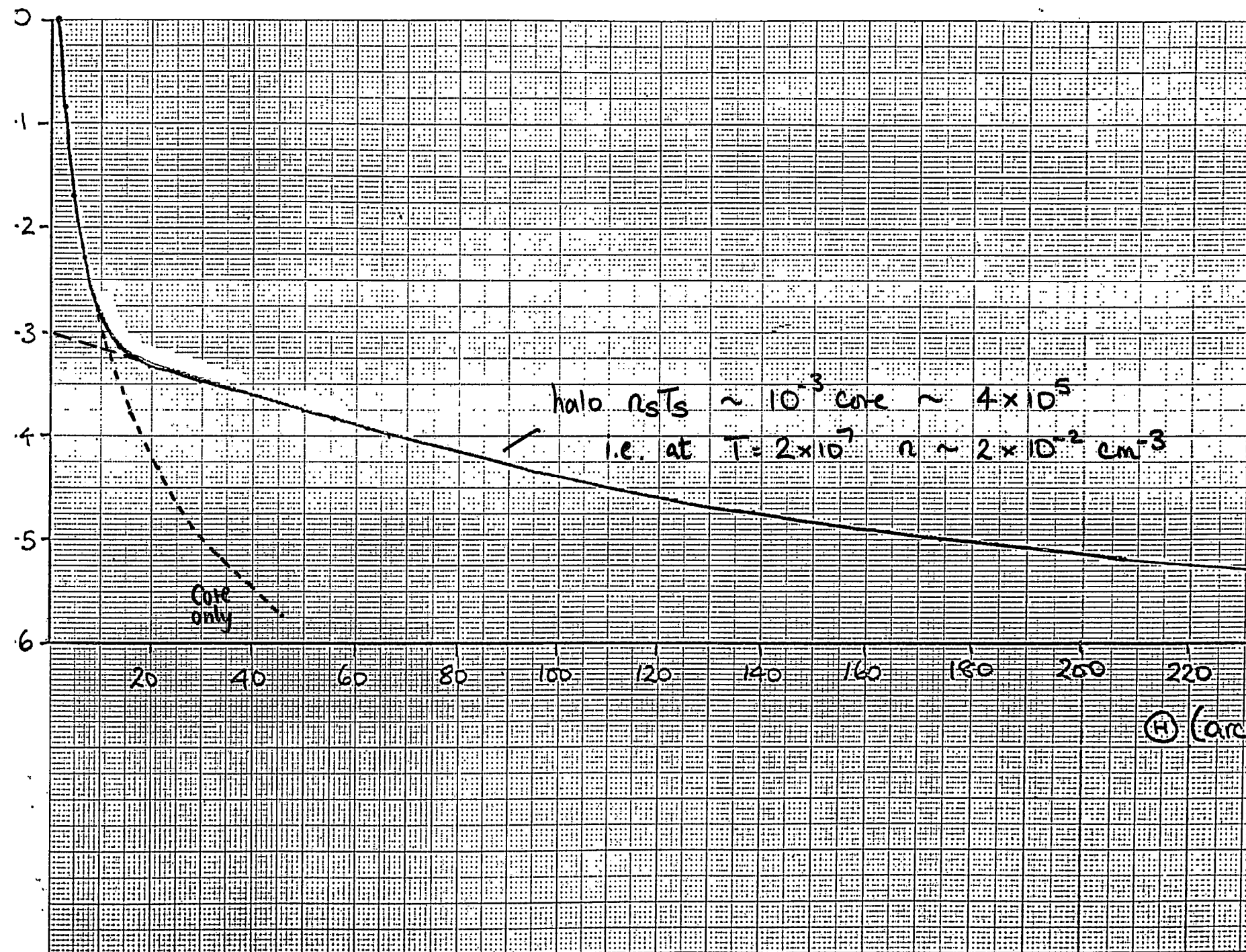


Table 4

Minimum Mass and 0.5-4 keV luminosity of media  
required to confine NGC6751 jet

| Assumed Isothermal Temp.                               | $4 \times 10^7$ K    | $2 \times 10^7$ K    | $10^7$ K             |
|--------------------------------------------------------|----------------------|----------------------|----------------------|
| $L_x(2.0 \text{ to } 50 \text{ kpc})$ , erg.s $^{-1}$  | $1.3 \times 10^{42}$ | $4.5 \times 10^{42}$ | $1.1 \times 10^{43}$ |
| $M(2.0 \text{ to } 50 \text{ kpc})$ , $M_\odot$        | $3.8 \times 10^{10}$ | $7.5 \times 10^{10}$ | $1.5 \times 10^{11}$ |
| $L_x(2.0 \text{ to } 200 \text{ kpc})$ , erg.s $^{-1}$ | $1.5 \times 10^{42}$ | $4.9 \times 10^{42}$ | $1.2 \times 10^{43}$ |
| $M(2.0 \text{ to } 200 \text{ kpc})$ , $M_\odot$       | $1.2 \times 10^{10}$ | $2.4 \times 10^{10}$ | $4.7 \times 10^{10}$ |
| $L_x(< 1.0 \text{ kpc})$ , erg.s $^{-1}$               | $4.7 \times 10^{43}$ | $1.6 \times 10^{44}$ | $3.8 \times 10^{44}$ |
| $M(< 1.0 \text{ kpc})$ , $M_\odot$                     | $7.6 \times 10^8$    | $1.5 \times 10^9$    | $3.0 \times 10^9$    |
| $L_x(< 2.0 \text{ kpc})$                               | $5.2 \times 10^{43}$ | $1.7 \times 10^{44}$ | $4.1 \times 10^{44}$ |
| $M(< 2.0 \text{ kpc})$                                 | $1.2 \times 10^9$    | $2.5 \times 10^9$    | $5.0 \times 10^9$    |

Converted to fm from Urq

15 April 1983

## Outflow limit from lobe Depth:

Willis, Wilson, Scrom (1978)  $\rightarrow$   $n_e$  in lobe  $< \cancel{2 \times 10^{-5}} \text{ cm}^{-3}$   
 $< 2 \times 10^5 \text{ m}^{-3}$   
 $B_{eq} = 1.5 \times 10^{-6} \text{ gauss.}$

$$\text{lobe radius} \sim 7.5' = 450'' = 193 \text{ kpc} = 5.96 \times 10^{21} \text{ m}$$

$$\begin{aligned}\text{Mass in sphere of this radius} &= \frac{4}{3} \pi \times 20 \times 1.67 \times 10^{-27} \times (5.96 \times 10^{21})^3 \\ &= 2.96 \times 10^{40} \text{ kg} \\ &= 1.5 \times 10^{10} M_\odot\end{aligned}$$

## Entrainment Upper Limit

$$\frac{dm}{dt dl} = 2\pi R_j \Sigma_{\text{ISM}} C_{\text{ISM}}$$

10" from core

$$\frac{nT}{T} \sim \frac{1.6 \times 10^5}{3 \times 10^7} \text{ cm}^{-3} \text{ K}$$

$$\rho = 2.2 \times 10^{-12} \text{ J/m}^3$$

$$n \sim 5.33 \times 10^{-3} \text{ cm}^{-3}$$

$$\rho = 8.9 \times 10^{-24} \text{ kg/m}^3$$

$$C_s = \sqrt{\frac{T\rho}{8}} = 6.4 \times 10^5 \text{ m/s} = 640 \text{ km/s}$$

$$R_j = 0.75, = 322 \text{ pc} = 9.93 \times 10^{18} \text{ m}$$

$$\text{Hence } \frac{dm}{dt dl} = 2 \times \pi \times 9.93 \times 10^{18} \times 8.9 \times 10^{-24} \times 6.4 \times 10^5 \text{ m/s}$$

$$= 3.55 \times 10^2 \text{ kg/sec.}$$

$$= 1.09 \times 10^{22} \text{ kg/kpc/sec}$$

$$= 3.46 \times 10^{23} \text{ kg/kpc/yr}$$

$$= \underline{\underline{0.17 M_\odot/\text{kpc/yr.}}}$$

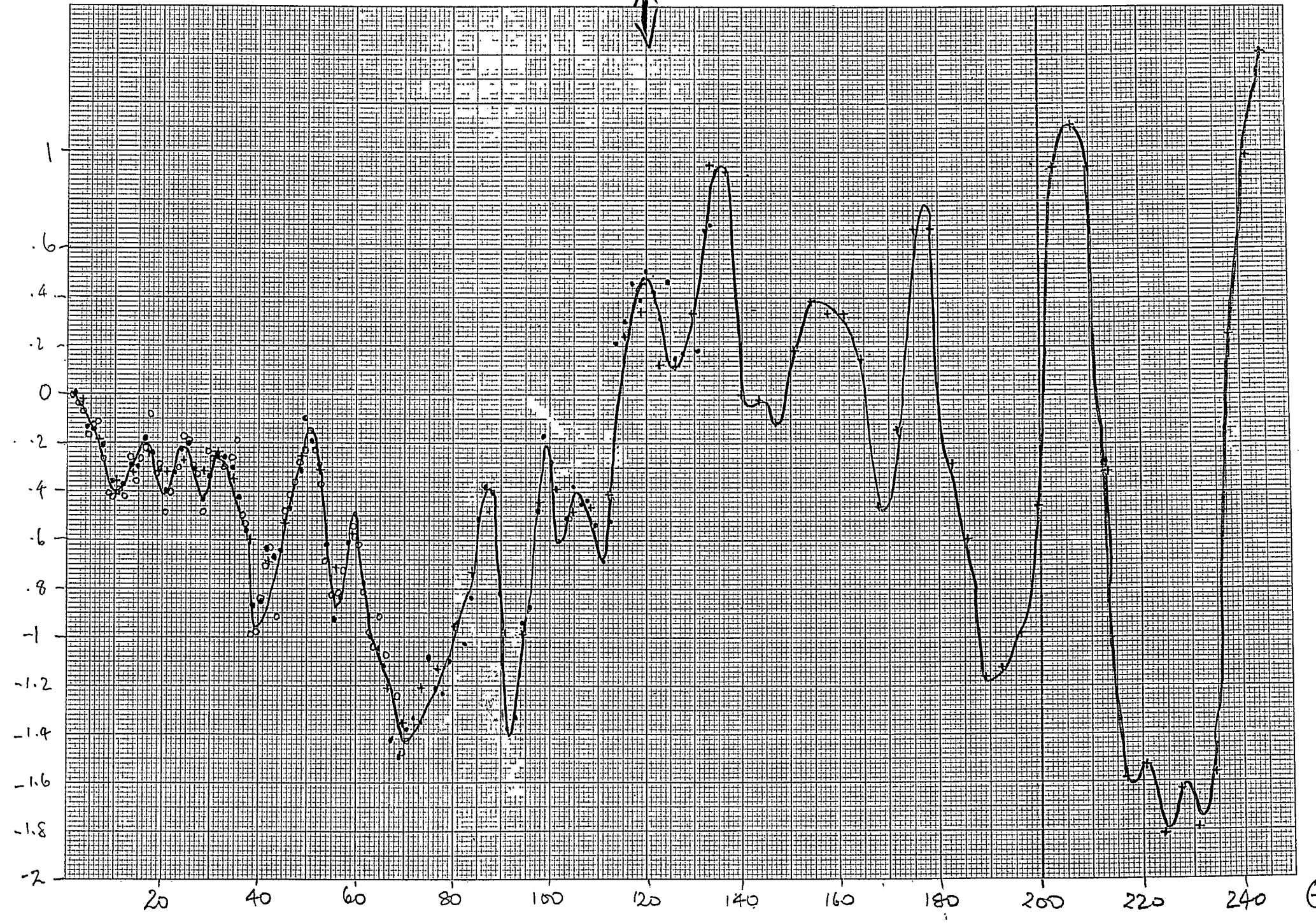
i.e. the length scale for entraining its own flow rate must be  $\gtrsim \frac{1.2 M_\odot/\text{yr}}{0.17 M_\odot/\text{kpc/yr}}$   
 $\gtrsim 7 \text{ kpc}$

i.e. velocity could be halved by  $\sim 7 \text{ kpc}$  further down the jet

i.e. by  $\theta \sim 26"$   $R_j = 1.84 \times R_{j,\text{in}}$

$\sigma < 150''$

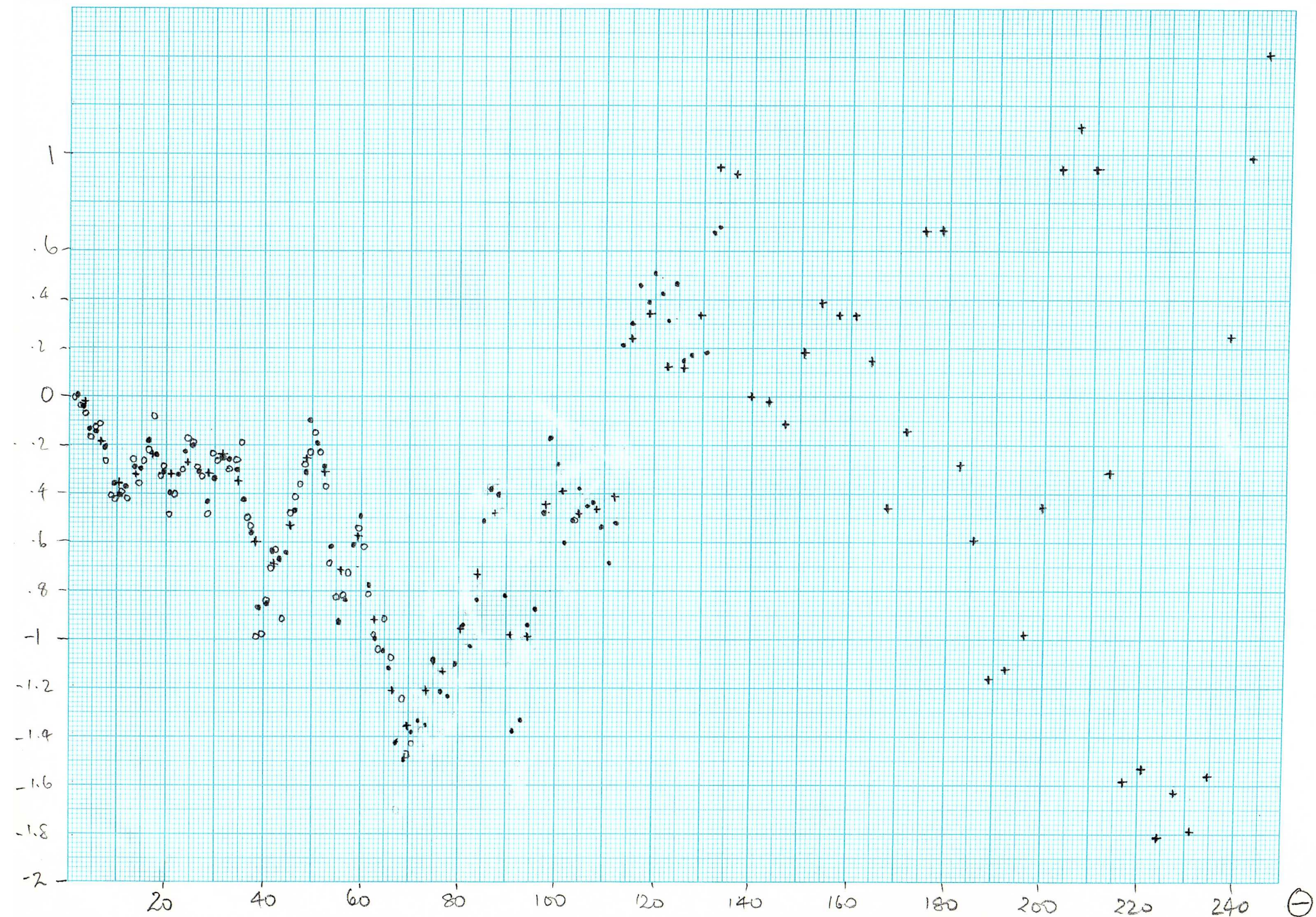
A



(E)

$\Delta < 150''$

A



(1)

Hanning Presitized

Power Sp. (S12) (Inner Jet)

1/3 dera  $\Delta(\theta)$  28" 17" 12.7 10.4 5.8  $\theta > 15.4$



$\Delta/\theta(\theta)$  25" 17.5 12.3 10.5 7.1 5.7  $\theta > 15.4$

(1024)

→ 27.8 16.9 9.0 5.8 (all)

(107.9 2026)

2/11 dera  $\Delta(\theta)$  37.5 17.3 9.1 12.1?  $15'' < \theta < 134''$

↑ ↑ ↑ ↓

26.5 18.? 9.1 12.5

$15'' < \theta < 100''$

$\Delta/\theta$  39.6 7.6 9.1 12.2 5.6  $15'' < \theta < 134''$

54.9 24.9 18.3 12.4 9.1

$15'' < \theta < 100''$

(all)

Conclude 9.1

12.4 growing  
17.6?

Averaged

$\Delta/\theta$  2" cell

$20'' < \theta < 60''$

17.5

11.8

9.0

17.8

11.4

9.5

17.3

11.6

8.7

17.1

11.5

8.7

6.9

$20'' < \theta < 80''$

$20'' < \theta < 100''$

$20'' < \theta < 120''$

Conclude  
finely

9.0, 12.1, 17.5

# Pawer Sp (S12) Outer Iter

|          |                         | too short |       |       |       |                 |
|----------|-------------------------|-----------|-------|-------|-------|-----------------|
| 15" defa | $\Delta(\theta)$        | 140"      | 35".5 | 28".0 |       | $\theta > 0$    |
|          |                         | 143"      |       | 27".3 |       | $\theta > 180"$ |
|          | $\Delta/\theta(\theta)$ | 146"      | 35".5 | 26".3 | 58".6 | $\theta > 0$    |
|          |                         | 144"      | 34".7 | 27".4 | 56"   | $\theta > 180"$ |

|          |                         |        |       |       |       |                 |      |                     |
|----------|-------------------------|--------|-------|-------|-------|-----------------|------|---------------------|
| 4.4 defa | $\Delta(\theta)$        | (137") | 31".2 | 23".3 | 17".1 | 12".6           | 5".4 | $\theta > 0$        |
|          | $\Delta(\theta)$        | (133") | 31".3 |       | 17".2 | 12".6           |      | $20 < \theta < 260$ |
|          | $\Delta/\theta(\theta)$ | (151") | 30".6 | 17".1 | 11".8 | <del>5".4</del> |      | $\theta > 0$        |
|          | $\Delta/\theta(\theta)$ | (140") | 31".3 | 17.2  | 12".7 | 58".0           |      | $20 < \theta < 260$ |



Conclude :    143"                57" ?.  
                     31".1  
                     17".2  
                     12".4

Overall      143"  
                 31".1  
                 17".5  
                 12".1  
                 9".0